Multiphysics in Haemodynamics: Fluid-Structure Interaction between Blood and Arterial Wall

Fabio Nobile

MOX, Politecnico di Milano

Joint work with: L. Formaggia, A. Moura, C. Vergara, MOX

Acknowledgements: P. Causin, J.F. Gerbeau

Workshop on Multiscale Problems, Cortona Sept. 18-22, 2006

Outline

1. Introduction
2. Mathematical problem
   - Governing equations
   - Global weak formulation
   - Energy inequality
3. Numerical approximation and stability analysis
   - ALE framework
   - Partitioned algorithms
   - Added mass effect
4. Absorbing boundary conditions
   - 1D hyperbolic model
   - Absorbing boundary conditions
5. Numerical results

Outline

1. Introduction
2. Mathematical problem
   - Governing equations
   - Global weak formulation
   - Energy inequality
3. Numerical approximation and stability analysis
   - ALE framework
   - Partitioned algorithms
   - Added mass effect
4. Absorbing boundary conditions
   - 1D hyperbolic model
   - Absorbing boundary conditions
5. Numerical results

Introduction

Local fluid dynamics is related to the development of vascular diseases

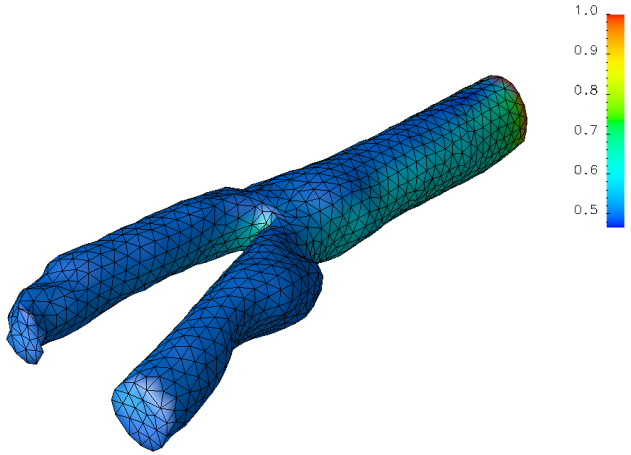

Peculiarities

- Pulsatile flow (heart beat $\sim 1sec$)
- Relatively large displacements
  $\Longrightarrow$ fluid domain movement non negligible
- Wave propagation due to fluid structure interaction
  $\Longrightarrow$ characteristic time: $t = \frac{L}{v} \approx \frac{0.25m}{5m/s} = 0.05sec$

Introduction

Local fluid dynamics is related to the development of vascular diseases

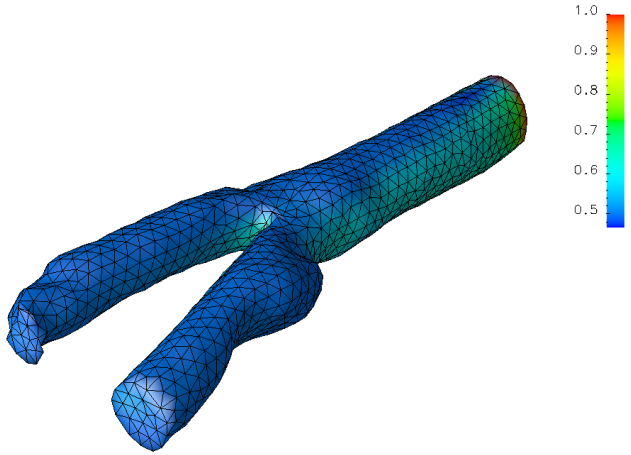

Peculiarities

- Pulsatile flow (heart beat $\sim 1sec$)
- Relatively large displacements
  $\Longrightarrow$ fluid domain movement non negligible
- Wave propagation due to fluid structure interaction
  $\Longrightarrow$ characteristic time: $t = \frac{L}{v} \approx \frac{0.25m}{5m/s} = 0.05sec$

Outline

1. Introduction
2. Mathematical problem
   - Governing equations
   - Global weak formulation
   - Energy inequality
3. Numerical approximation and stability analysis
   - ALE framework
   - Partitioned algorithms
   - Added mass effect
4. Absorbing boundary conditions
   - 1D hyperbolic model
   - Absorbing boundary conditions
5. Numerical results

Physical Model

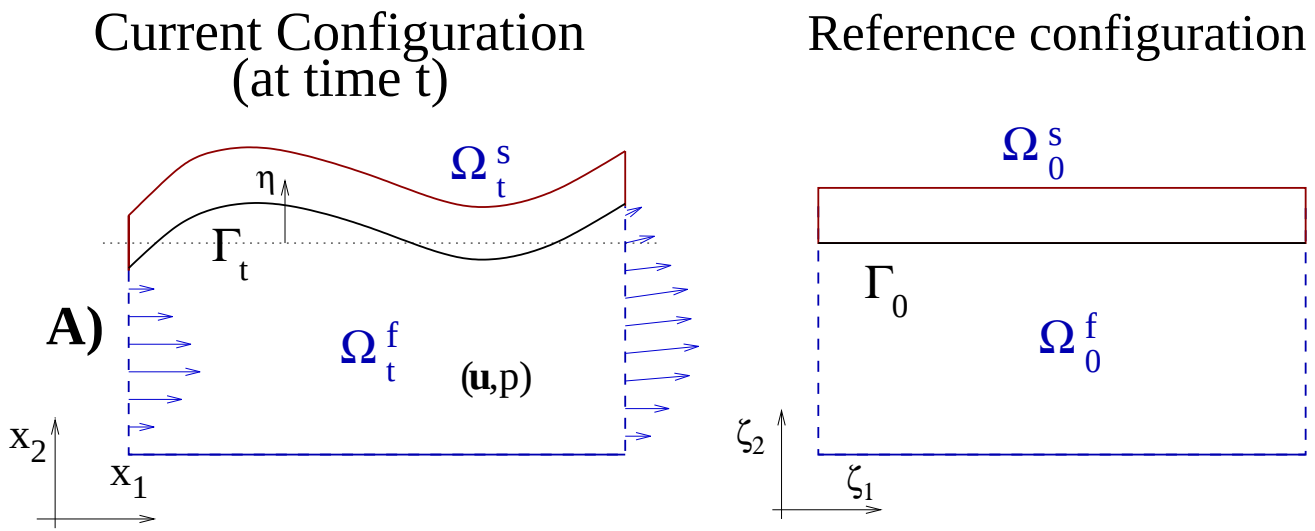

- Fluid equations defined in the moving domain Ω_t^f. Typically written in Eulerian form
- Structure equations typically written in Lagrangian form on the reference domain Ω_0^s.

Physical Model

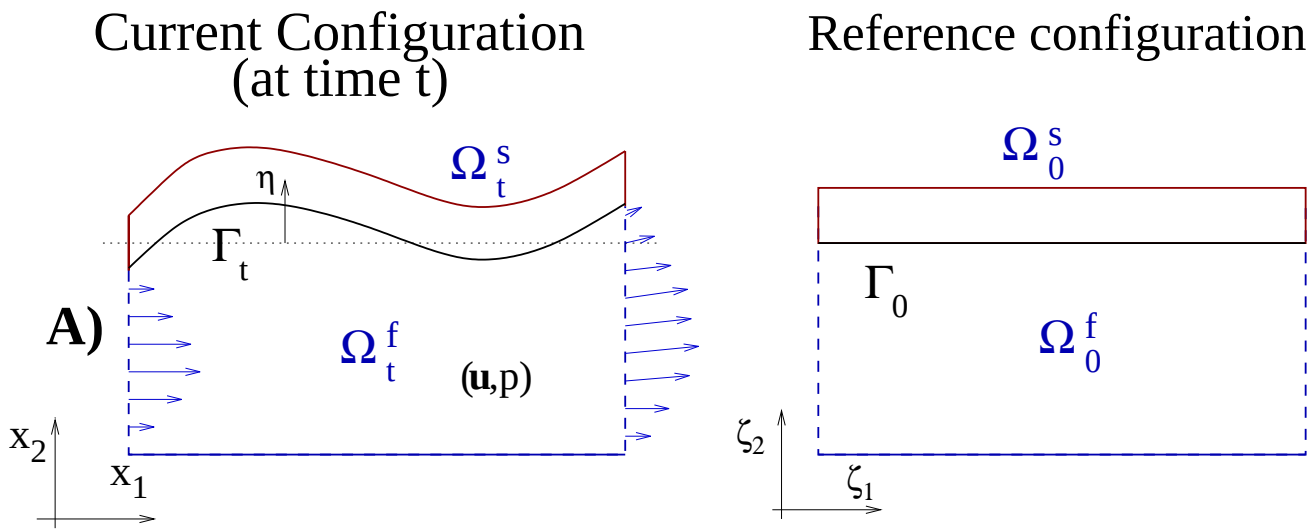

- Fluid equations defined in the moving domain Ω_t^f. Typically written in Eulerian form
- Structure equations typically written in Lagrangian form on the reference domain Ω_0^s.

Physical Model – Fluid

•Blood can be treated as a homogeneous, incompressible, Newtonian fluid in large arteries.

Navier-Stokes equations

$$\begin{cases} \varrho_f \dfrac{\partial \mathbf{u}}{\partial t} + \varrho_f \operatorname{div}(\mathbf{u} \otimes \mathbf{u}) - \operatorname{div} \boldsymbol{\sigma}_\mathbf{f}(\mathbf{u}, p) = \mathbf{f}^f \\ \operatorname{div} \mathbf{u} = 0 \\ + \text{ suitable initial and boundary conditions} \end{cases} \quad \text{in } \Omega_t^f,$$

$\mathbf{u}$: fluid velocity

$\mathbf{D}(\mathbf{u}) = \frac{\nabla \mathbf{u} + \nabla^T \mathbf{u}}{2}$: strain tensor

p: fluid pressure

$\boldsymbol{\sigma}_\mathbf{f}(\mathbf{u}, p) = 2\mu \mathbf{D}(\mathbf{u}) - p\mathbf{I}$: fluid stress tensor

Physical Model – Structure

- Arteries are (relatively) thin, multilayered structures, which deform principally in the radial direction.
- Deformations can reach up to 10% of the artery diameter
- Several models have been proposed: 3D non-linear elasticity, shell (membrane) models, simplified models only for radial displacement.

Non-linear elasticity

Unknown: Structure displacement $\eta(t, \xi) = \mathbf{x}(t, \xi) - \xi$

Physical Model – Structure

- Arteries are (relatively) thin, multilayered structures, which deform principally in the radial direction.
- Deformations can reach up to 10% of the artery diameter
- Several models have been proposed: 3D non-linear elasticity, shell (membrane) models, simplified models only for radial displacement.

Non-linear elasticity

Unknown: Structure displacement $\eta(t, \xi) = \mathbf{x}(t, \xi) - \xi$

Physical Model – Structure

- Arteries are (relatively) thin, multilayered structures, which deform principally in the radial direction.
- Deformations can reach up to 10% of the artery diameter
- Several models have been proposed: 3D non-linear elasticity, shell (membrane) models, simplified models only for radial displacement.

Non-linear elasticity

Unknown: Structure displacement $\eta(t, \xi) = \mathbf{x}(t, \xi) - \xi$

Physical Model – Structure

- Arteries are (relatively) thin, multilayered structures, which deform principally in the radial direction.
- Deformations can reach up to 10% of the artery diameter
- Several models have been proposed: 3D non-linear elasticity, shell (membrane) models, simplified models only for radial displacement.

Non-linear elasticity

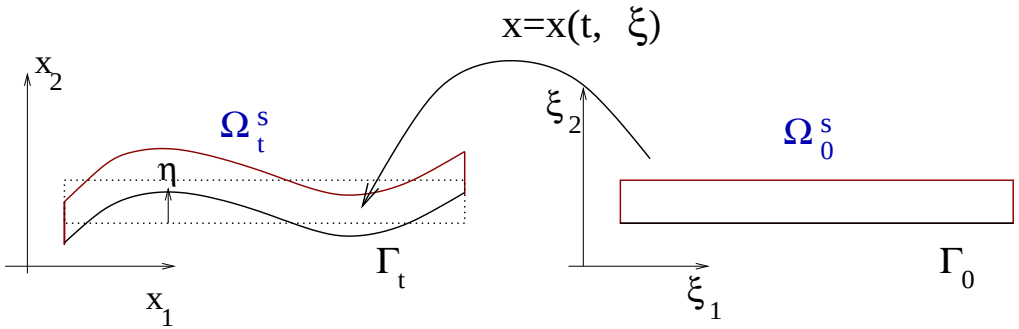

Unknown: Structure displacement $\eta(t, \xi) = \mathbf{x}(t, \xi) - \xi$

Physical Model – Structure

Non-linear elasticity

$$\varrho_s^0 \frac{\partial^2 \boldsymbol{\eta}}{\partial t^2} - \mathrm{div}_0 \left[\mathbf{F}(\boldsymbol{\eta}) \mathbf{S}(\boldsymbol{\eta}) \right] = f_0^s, \quad \text{in } \Omega_0^s,$$

where $\mathbf{F} = \mathbf{I} + \nabla_0 \boldsymbol{\eta}$: deformation gradient

$J(\boldsymbol{\eta}) = \det(F(\boldsymbol{\eta}))$: change of volume

$\mathbf{E} = \frac{1}{2}(\mathbf{F}^T \mathbf{F} - \mathbf{I})$: Green strain tensor

$\mathbf{S}$: second Piola-Kirchhoff stress tensor

Constitutive law

Hyperelastic materials $\mathbf{S} = \frac{\partial W(\mathbf{E})}{\partial \mathbf{E}}$, ($W$: elastic energy)

St. Venant-Kirchhoff materials $\mathbf{S} = \lambda \, \mathrm{tr}(\mathbf{E}) \mathbf{I} + 2\mu \mathbf{E}$

Physical Model – Structure

Non-linear elasticity

$$\varrho_s^0 \frac{\partial^2 \boldsymbol{\eta}}{\partial t^2} - \mathrm{div}_0 \left[\mathbf{F}(\boldsymbol{\eta}) \mathbf{S}(\boldsymbol{\eta}) \right] = f_0^s, \quad \text{in } \Omega_0^s,$$

where $\mathbf{F} = \mathbf{I} + \nabla_0 \boldsymbol{\eta}$: deformation gradient

$J(\boldsymbol{\eta}) = \det(F(\boldsymbol{\eta}))$: change of volume

$\mathbf{E} = \frac{1}{2}(\mathbf{F}^T \mathbf{F} - \mathbf{I})$: Green strain tensor

$\mathbf{S}$: second Piola-Kirchhoff stress tensor

Constitutive law

Hyperelastic materials $\quad \mathbf{S} = \frac{\partial W(\mathbf{E})}{\partial \mathbf{E}}, \qquad (W\text{: elastic energy})$

St. Venant-Kirchhoff materials $\quad \mathbf{S} = \lambda \, \mathrm{tr}(\mathbf{E}) \mathbf{I} + 2\mu \mathbf{E}$

Physical Model – Coupling conditions

On reference interface Γ_0

- Continuity of velocity (kinematic condition)

$$\mathbf{u} \circ \mathbf{x}(\boldsymbol{\xi}) = \frac{\partial \boldsymbol{\eta}}{\partial t}$$

- Continuity of normal stress (dynamic condition)

$$J(\boldsymbol{\eta})\boldsymbol{\sigma}_f(\mathbf{u}, p)F^{-T}(\boldsymbol{\eta})\mathbf{n}_0^f = -F(\boldsymbol{\eta})S(\boldsymbol{\eta})\mathbf{n}_0^s$$

with $\mathbf{n}_0^f = -\mathbf{n}_0^s$.

Physical Model – Coupling conditions

On reference interface Γ_0

- Continuity of velocity (kinematic condition)

$$\mathbf{u} \circ \mathbf{x}(\boldsymbol{\xi}) = \frac{\partial \boldsymbol{\eta}}{\partial t}$$

- Continuity of normal stress (dynamic condition)

$$J(\boldsymbol{\eta})\boldsymbol{\sigma}_f(\mathbf{u}, p)F^{-T}(\boldsymbol{\eta})\mathbf{n}_0^f = -F(\boldsymbol{\eta})S(\boldsymbol{\eta})\mathbf{n}_0^s$$

with $\mathbf{n}_0^f = -\mathbf{n}_0^s$.

A global weak formulation

Fluid eqs. Multiply by $(v, q) \in \mathbf{H}^1_{\Gamma_D}(\Omega^f_t) \times L^2(\Omega^f_t)$

$$\int_{\Omega^f_t} \varrho_f \left(\frac{\partial \mathbf{u}}{\partial t} + \mathrm{div}(\mathbf{u} \otimes \mathbf{u}) \right) \cdot \mathbf{v} + \boldsymbol{\sigma}_f : \nabla \mathbf{v} + \mathrm{div}\, \mathbf{u} q = \int_{\Omega^f_t} \mathbf{f}^f \cdot \mathbf{v} + \int_{\Gamma_t} (\boldsymbol{\sigma}_f \cdot \mathbf{n}^f) \cdot \mathbf{v}$$

Structure eq. Multiply by $\phi \in \mathbf{H}^1_{\Gamma_D}(\Omega^s_0)$

$$\int_{\Omega^s_0} \varrho^0_s \frac{\partial^2 \boldsymbol{\eta}}{\partial t^2} \cdot \phi + \mathbf{F}(\boldsymbol{\eta}) \mathbf{S}(\boldsymbol{\eta}) : \nabla_0 \phi = \int_{\Omega^s_0} f^s_0 \cdot \phi + \int_{\Gamma_0} (\mathbf{F}(\boldsymbol{\eta}) \mathbf{S}(\boldsymbol{\eta}) \cdot \mathbf{n}^s_0) \cdot \phi$$

Global weak formulation - cont.

•If we take matching test functions at the interface: $\mathbf{v} \circ \mathbf{x}(\boldsymbol{\xi}) = \boldsymbol{\phi}(\boldsymbol{\xi})$ and thanks to the coupling condition (continuity of stresses), the interface terms perfectly cancel.

Fluid-Structure functional space

$$V \equiv \{(\mathbf{v}, q, \boldsymbol{\phi}) : \ \mathbf{v} \circ \mathbf{x}(\boldsymbol{\xi}) = \boldsymbol{\phi}(\boldsymbol{\xi}) \ \text{ on } \Gamma_0\}$$

$$\int_{\Omega_t^f} \varrho_f \left(\frac{\partial \mathbf{u}}{\partial t} + \operatorname{div}(\mathbf{u} \otimes \mathbf{u}) \right) \cdot \mathbf{v} + \boldsymbol{\sigma}_f(\mathbf{u}, p) : \nabla \mathbf{v} + \operatorname{div} \mathbf{u} q +$$

$$\int_{\Omega_0^s} \varrho_s^0 \frac{\partial^2 \boldsymbol{\eta}}{\partial t^2} \cdot \boldsymbol{\phi} + \mathbf{F}(\boldsymbol{\eta}) \mathbf{S}(\boldsymbol{\eta}) : \nabla_0 \boldsymbol{\phi} = \int_{\Omega_t^f} \mathbf{f}^f \cdot \mathbf{v} + \int_{\Omega_0^s} f_0^s \cdot \boldsymbol{\phi}$$

$+$ coupling condition $\mathbf{u} \circ \mathbf{x}(\boldsymbol{\xi}) = \frac{\partial \boldsymbol{\eta}}{\partial t}$

Global weak formulation - cont.

•If we take matching test functions at the interface: $\mathbf{v} \circ \mathbf{x}(\boldsymbol{\xi}) = \boldsymbol{\phi}(\boldsymbol{\xi})$ and thanks to the coupling condition (continuity of stresses), the interface terms perfectly cancel.

Fluid-Structure functional space

$$V \equiv \{(\mathbf{v}, q, \boldsymbol{\phi}) : \ \mathbf{v} \circ \mathbf{x}(\boldsymbol{\xi}) = \boldsymbol{\phi}(\boldsymbol{\xi}) \ \text{ on } \Gamma_0\}$$

$$\int_{\Omega_t^f} \varrho_f \left(\frac{\partial \mathbf{u}}{\partial t} + \operatorname{div}(\mathbf{u} \otimes \mathbf{u}) \right) \cdot \mathbf{v} + \boldsymbol{\sigma}_f(\mathbf{u}, p) : \nabla \mathbf{v} + \operatorname{div} \mathbf{u} q +$$

$$\int_{\Omega_0^s} \varrho_s^0 \frac{\partial^2 \boldsymbol{\eta}}{\partial t^2} \cdot \boldsymbol{\phi} + \mathbf{F}(\boldsymbol{\eta}) \mathbf{S}(\boldsymbol{\eta}) : \nabla_0 \boldsymbol{\phi} = \int_{\Omega_t^f} \mathbf{f}^f \cdot \mathbf{v} + \int_{\Omega_0^s} f_0^s \cdot \boldsymbol{\phi}$$

$+$ coupling condition $\mathbf{u} \circ \mathbf{x}(\boldsymbol{\xi}) = \frac{\partial \boldsymbol{\eta}}{\partial t}$

Global weak formulation - cont.

•If we take matching test functions at the interface: $\mathbf{v} \circ \mathbf{x}(\boldsymbol{\xi}) = \boldsymbol{\phi}(\boldsymbol{\xi})$ and thanks to the coupling condition (continuity of stresses), the interface terms perfectly cancel.

Fluid-Structure functional space

$$V \equiv \{(\mathbf{v}, q, \boldsymbol{\phi}) : \ \mathbf{v} \circ \mathbf{x}(\boldsymbol{\xi}) = \boldsymbol{\phi}(\boldsymbol{\xi}) \ \text{ on } \Gamma_0\}$$

$$\int_{\Omega_t^f} \varrho_f \left(\frac{\partial \mathbf{u}}{\partial t} + \operatorname{div}(\mathbf{u} \otimes \mathbf{u}) \right) \cdot \mathbf{v} + \boldsymbol{\sigma}_f(\mathbf{u}, p) : \nabla \mathbf{v} + \operatorname{div} \mathbf{u} q +$$

$$\int_{\Omega_0^s} \varrho_s^0 \frac{\partial^2 \boldsymbol{\eta}}{\partial t^2} \cdot \boldsymbol{\phi} + \mathbf{F}(\boldsymbol{\eta}) \mathbf{S}(\boldsymbol{\eta}) : \nabla_0 \boldsymbol{\phi} = \int_{\Omega_t^f} \mathbf{f}^f \cdot \mathbf{v} + \int_{\Omega_0^s} f_0^s \cdot \boldsymbol{\phi}$$

$+$ coupling condition $\mathbf{u} \circ \mathbf{x}(\boldsymbol{\xi}) = \frac{\partial \boldsymbol{\eta}}{\partial t}$

Energy inequality

•Taking as test functions $(\mathbf{v}, q, \phi) = (\mathbf{u}, p, \dot{\boldsymbol{\eta}})$ we can derive an Energy inequality

Fluid Structure Energy (kinetic + elastic)

$$\mathcal{E}(t) \equiv \frac{\varrho_f}{2}\|\mathbf{u}(t)\|^2_{L^2(\Omega^f_t)} + \frac{\varrho^s_0}{2}\|\frac{\partial \boldsymbol{\eta}}{\partial t}(t)\|^2_{L^2(\Omega^s_0)} + \int_{\Omega^s_0} W(\boldsymbol{\eta})(t)$$

Then (homogeneous problem)

$$\mathcal{E}_{FS}(T) + 2\mu \int_0^T \int_{\Omega^f_t} \mathbf{D}(\mathbf{u}) : \mathbf{D}(\mathbf{u})\, d\Omega\, dt \;\leq\; \mathcal{E}_{FS}(0)$$

Energy inequality

•Taking as test functions $(\mathbf{v}, q, \phi) = (\mathbf{u}, p, \dot{\boldsymbol{\eta}})$ we can derive an Energy inequality

Fluid Structure Energy (kinetic + elastic)

$$\mathcal{E}(t) \equiv \frac{\varrho_f}{2}\|\mathbf{u}(t)\|^2_{L^2(\Omega^f_t)} + \frac{\varrho^s_0}{2}\|\frac{\partial \boldsymbol{\eta}}{\partial t}(t)\|^2_{L^2(\Omega^s_0)} + \int_{\Omega^s_0} W(\boldsymbol{\eta})(t)$$

Then (homogeneous problem)

$$\mathcal{E}_{FS}(T) + 2\mu \int_0^T \int_{\Omega^f_t} \mathbf{D}(\mathbf{u}) : \mathbf{D}(\mathbf{u})\, d\Omega\, dt \;\leq\; \mathcal{E}_{FS}(0)$$

Energy inequality

•Taking as test functions $(\mathbf{v}, q, \phi) = (\mathbf{u}, p, \dot{\boldsymbol{\eta}})$ we can derive an Energy inequality

Fluid Structure Energy (kinetic + elastic)

$$\mathcal{E}(t) \equiv \frac{\varrho_f}{2}\|\mathbf{u}(t)\|^2_{L^2(\Omega^f_t)} + \frac{\varrho^s_0}{2}\|\frac{\partial \boldsymbol{\eta}}{\partial t}(t)\|^2_{L^2(\Omega^s_0)} + \int_{\Omega^s_0} W(\boldsymbol{\eta})(t)$$

Then (homogeneous problem)

$$\mathcal{E}_{FS}(T) + 2\mu \int_0^T \int_{\Omega^f_t} \mathbf{D}(\mathbf{u}) : \mathbf{D}(\mathbf{u})\, d\Omega\, dt \quad \leq \quad \mathcal{E}_{FS}(0)$$

Energy Inequality

Key points in deriving an energy inequality:

- Perfect balance of work at the interface

$$\int_{\Gamma_t} (\boldsymbol{\sigma}_f \cdot \mathbf{n}^f) \cdot \mathbf{u} = -\int_{\Gamma_0} (\mathbf{F}(\eta)\mathbf{S}(\eta) \cdot \mathbf{n}_0^s) \cdot \frac{\partial \eta}{\partial t}$$

- No kinetic flux through the interface

$$\text{(time der.)} \qquad \int_{\Omega_t^f} \varrho_f \frac{\partial \mathbf{u}}{\partial t} \cdot \mathbf{u} = \frac{\varrho_f}{2} \frac{d}{dt} \int_{\Omega_t^f} |\mathbf{u}|^2 - \frac{\varrho_f}{2} \int_{\Gamma_t} |\mathbf{u}^2| \mathbf{w} \cdot \mathbf{n}$$

$$\text{(convective term)} \qquad \int_{\Omega_t^f} \varrho_f \operatorname{div}(\mathbf{u} \otimes \mathbf{u}) \cdot \mathbf{u} = \frac{\varrho_f}{2} \int_{\Gamma_t} |\mathbf{u}^2| \mathbf{u} \cdot \mathbf{n}$$

where $\mathbf{w}$ is the velocity at which the interface moves.
Since $\mathbf{w} = \mathbf{u} = \dot{\eta}$, the kinetic flux $\frac{\varrho_f}{2} \int_{\Gamma_t} |\mathbf{u}^2|(\mathbf{u} - \mathbf{w}) \cdot \mathbf{n}$ vanishes.

- This does not hold if one couples Stokes with a non-linear structure

Energy Inequality

Key points in deriving an energy inequality:

- Perfect balance of work at the interface

$$\int_{\Gamma_t} (\boldsymbol{\sigma}_f \cdot \mathbf{n}^f) \cdot \mathbf{u} = -\int_{\Gamma_0} (\mathbf{F}(\eta)\mathbf{S}(\eta) \cdot \mathbf{n}_0^s) \cdot \frac{\partial \eta}{\partial t}$$

- No kinetic flux through the interface

$$\text{(time der.)} \qquad \int_{\Omega_t^f} \varrho_f \frac{\partial \mathbf{u}}{\partial t} \cdot \mathbf{u} = \frac{\varrho_f}{2} \frac{d}{dt} \int_{\Omega_t^f} |\mathbf{u}|^2 - \frac{\varrho_f}{2} \int_{\Gamma_t} |\mathbf{u}^2| \mathbf{w} \cdot \mathbf{n}$$

$$\text{(convective term)} \qquad \int_{\Omega_t^f} \varrho_f \operatorname{div}(\mathbf{u} \otimes \mathbf{u}) \cdot \mathbf{u} = \frac{\varrho_f}{2} \int_{\Gamma_t} |\mathbf{u}^2| \mathbf{u} \cdot \mathbf{n}$$

where $\mathbf{w}$ is the velocity at which the interface moves.
Since $\mathbf{w} = \mathbf{u} = \dot{\eta}$, the kinetic flux $\frac{\varrho_f}{2} \int_{\Gamma_t} |\mathbf{u}^2|(\mathbf{u} - \mathbf{w}) \cdot \mathbf{n}$ vanishes.

- This does not hold if one couples Stokes with a non-linear structure

Energy Inequality

Key points in deriving an energy inequality:

- Perfect balance of work at the interface

$$\int_{\Gamma_t} (\boldsymbol{\sigma}_f \cdot \mathbf{n}^f) \cdot \mathbf{u} = - \int_{\Gamma_0} (\mathbf{F}(\eta)\mathbf{S}(\eta) \cdot \mathbf{n}_0^s) \cdot \frac{\partial \eta}{\partial t}$$

- No kinetic flux through the interface

(time der.) $$\int_{\Omega_t^f} \varrho_f \frac{\partial \mathbf{u}}{\partial t} \cdot \mathbf{u} = \frac{\varrho_f}{2} \frac{d}{dt} \int_{\Omega_t^f} |\mathbf{u}|^2 - \frac{\varrho_f}{2} \int_{\Gamma_t} |\mathbf{u}^2| \mathbf{w} \cdot \mathbf{n}$$

(convective term) $$\int_{\Omega_t^f} \varrho_f \operatorname{div}(\mathbf{u} \otimes \mathbf{u}) \cdot \mathbf{u} = \frac{\varrho_f}{2} \int_{\Gamma_t} |\mathbf{u}^2| \mathbf{u} \cdot \mathbf{n}$$

where $\mathbf{w}$ is the velocity at which the interface moves.
Since $\mathbf{w} = \mathbf{u} = \dot{\eta}$, the kinetic flux $\frac{\varrho_f}{2} \int_{\Gamma_t} |\mathbf{u}^2| (\mathbf{u} - \mathbf{w}) \cdot \mathbf{n}$ vanishes.

- This does not hold if one couples Stokes with a non-linear structure

Other structure models

- Assuming a cylindrical reference configuration, simpler models have been proposed, accounting only for radial displacement $\boldsymbol{\eta} : \Gamma_0 \longrightarrow \mathbb{R}$. They reproduce correctly the pressure wave propagation.

  Independent ring: $\varrho_0^s h_s \dfrac{\partial^2 \eta}{\partial t^2} + \dfrac{E h_s}{(1-\nu^2) R_0^2} \eta = f_s$

  Algebraic law: $\dfrac{E h_s}{(1-\nu^2) R_0^2} \eta = f_s$

  Coupling conditions: $\mathbf{u} \circ \mathbf{x}(\boldsymbol{\xi}) = \dfrac{\partial \eta}{\partial t} \mathbf{e}_r, \qquad f_s = \mathbf{e}_r^T \left[J \boldsymbol{\sigma}_{\mathbf{f}}(\mathbf{u}, p) F_t^{-T} \right] \mathbf{e}_r$
- Global weak formulations and energy inequalities can be derived in these cases as well
- Well posedness. Only partial results available even for 2D problems and simple structure models. (Y. Maday, C. Grandmont, B. Desjardens, M, Esteban, H. Beirao da Veiga, D. Coutand, ...)

Other structure models

- Assuming a cylindrical reference configuration, simpler models have been proposed, accounting only for radial displacement $\boldsymbol{\eta} : \Gamma_0 \longrightarrow \mathbb{R}$. They reproduce correctly the pressure wave propagation.

Independent ring: $$\varrho_0^s h_s \frac{\partial^2 \eta}{\partial t^2} + \frac{E h_s}{(1-\nu^2) R_0^2} \eta = f_s$$

Algebraic law: $$\frac{E h_s}{(1-\nu^2) R_0^2} \eta = f_s$$

Coupling conditions: $\mathbf{u} \circ \mathbf{x}(\boldsymbol{\xi}) = \frac{\partial \eta}{\partial t} \mathbf{e}_r, \qquad f_s = \mathbf{e}_r^T \left[J \boldsymbol{\sigma}_{\mathbf{f}}(\mathbf{u}, p) F_t^{-T} \right] \mathbf{e}_r$

- Global weak formulations and energy inequalities can be derived in these cases as well
- Well posedness. Only partial results available even for 2D problems and simple structure models. (Y. Maday, C. Grandmont, B. Desjardens, M, Esteban, H. Beirao da Veiga, D. Coutand, ...)

Other structure models

- Assuming a cylindrical reference configuration, simpler models have been proposed, accounting only for radial displacement $\boldsymbol{\eta} : \Gamma_0 \longrightarrow \mathbb{R}$. They reproduce correctly the pressure wave propagation.

Independent ring: $$\varrho_0^s h_s \frac{\partial^2 \eta}{\partial t^2} + \frac{E h_s}{(1-\nu^2) R_0^2} \eta = f_s$$

Algebraic law: $$\frac{E h_s}{(1-\nu^2) R_0^2} \eta = f_s$$

Coupling conditions: $\mathbf{u} \circ \mathbf{x}(\boldsymbol{\xi}) = \frac{\partial \eta}{\partial t} \mathbf{e}_r, \qquad f_s = \mathbf{e}_r^T \left[J \boldsymbol{\sigma}_{\mathbf{f}}(\mathbf{u}, p) F_t^{-T} \right] \mathbf{e}_r$

- Global weak formulations and energy inequalities can be derived in these cases as well
- Well posedness. Only partial results available even for 2D problems and simple structure models. (Y. Maday, C. Grandmont, B. Desjardens, M, Esteban, H. Beirao da Veiga, D. Coutand, ...)

Other structure models

- Assuming a cylindrical reference configuration, simpler models have been proposed, accounting only for radial displacement $\boldsymbol{\eta} : \Gamma_0 \longrightarrow \mathbb{R}$. They reproduce correctly the pressure wave propagation.

  Independent ring: $$\varrho_0^s h_s \frac{\partial^2 \eta}{\partial t^2} + \frac{E h_s}{(1-\nu^2) R_0^2} \eta = f_s$$

  Algebraic law: $$\frac{E h_s}{(1-\nu^2) R_0^2} \eta = f_s$$

  Coupling conditions: $\mathbf{u} \circ \mathbf{x}(\boldsymbol{\xi}) = \frac{\partial \eta}{\partial t} \mathbf{e}_r, \qquad f_s = \mathbf{e}_r^T \left[J \boldsymbol{\sigma}_{\mathbf{f}}(\mathbf{u}, p) F_t^{-T} \right] \mathbf{e}_r$
- Global weak formulations and energy inequalities can be derived in these cases as well
- Well posedness. Only partial results available even for 2D problems and simple structure models. (Y. Maday, C. Grandmont, B. Desjardens, M, Esteban, H. Beirao da Veiga, D. Coutand, ...)

Other structure models

- Assuming a cylindrical reference configuration, simpler models have been proposed, accounting only for radial displacement $\boldsymbol{\eta} : \Gamma_0 \longrightarrow \mathbb{R}$. They reproduce correctly the pressure wave propagation.

  Independent ring: $$\varrho_0^s h_s \frac{\partial^2 \eta}{\partial t^2} + \frac{E h_s}{(1-\nu^2) R_0^2} \eta = f_s$$

  Algebraic law: $$\frac{E h_s}{(1-\nu^2) R_0^2} \eta = f_s$$

  Coupling conditions: $\mathbf{u} \circ \mathbf{x}(\boldsymbol{\xi}) = \frac{\partial \eta}{\partial t} \mathbf{e}_r, \qquad f_s = \mathbf{e}_r^T \left[J \boldsymbol{\sigma}_{\mathbf{f}}(\mathbf{u}, p) F_t^{-T} \right] \mathbf{e}_r$
- Global weak formulations and energy inequalities can be derived in these cases as well
- Well posedness. Only partial results available even for 2D problems and simple structure models. (Y. Maday, C. Grandmont, B. Desjardens, M, Esteban, H. Beirao da Veiga, D. Coutand, ...)

Other structure models

- Assuming a cylindrical reference configuration, simpler models have been proposed, accounting only for radial displacement $\boldsymbol{\eta} : \Gamma_0 \longrightarrow \mathbb{R}$. They reproduce correctly the pressure wave propagation.

  Independent ring: $$\varrho_0^s h_s \frac{\partial^2 \eta}{\partial t^2} + \frac{E h_s}{(1-\nu^2) R_0^2} \eta = f_s$$

  Algebraic law: $$\frac{E h_s}{(1-\nu^2) R_0^2} \eta = f_s$$

  Coupling conditions: $\mathbf{u} \circ \mathbf{x}(\boldsymbol{\xi}) = \frac{\partial \eta}{\partial t} \mathbf{e}_r, \qquad f_s = \mathbf{e}_r^T \left[J \boldsymbol{\sigma}_\mathbf{f}(\mathbf{u}, p) F_t^{-T} \right] \mathbf{e}_r$
- Global weak formulations and energy inequalities can be derived in these cases as well
- Well posedness. Only partial results available even for 2D problems and simple structure models. (Y. Maday, C. Grandmont, B. Desjardens, M, Esteban, H. Beirao da Veiga, D. Coutand, ...)

Outline

1. Introduction
2. Mathematical problem
   - Governing equations
   - Global weak formulation
   - Energy inequality
3. Numerical approximation and stability analysis
   - ALE framework
   - Partitioned algorithms
   - Added mass effect
4. Absorbing boundary conditions
   - 1D hyperbolic model
   - Absorbing boundary conditions
5. Numerical results

Numerical Approximation

•Space discretization by Finite Elements both for the fluid and the structure.

Major difficulties

- Discretize fluid equations on a moving domain $\Rightarrow$ ALE formulation
- Find stable time discretization schemes and coupling strategies.

ALE Formulation

- The moving domain is recast at each time t to a fixed configuration Ω_0^f through the ALE mapping $\mathcal{A}_t$:

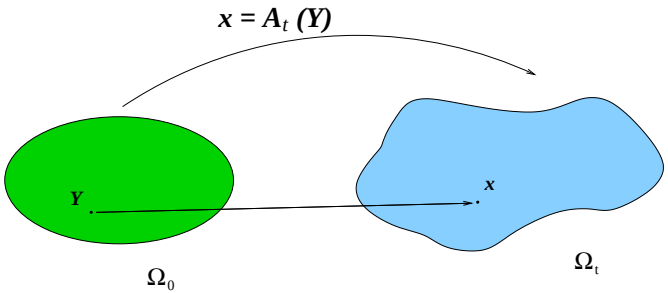

$$\mathcal{A}_t : \Omega_0 \longrightarrow \Omega_t,$$
$$\mathbf{x}(\boldsymbol{\xi}, t) = \mathcal{A}_t(\boldsymbol{\xi})$$

ALE Formulation

- The moving domain is recast at each time t to a fixed configuration Ω_0^f through the ALE mapping $\mathcal{A}_t$:

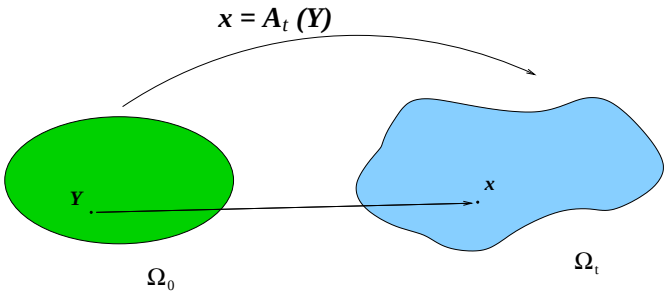

$$\mathcal{A}_t : \Omega_0 \longrightarrow \Omega_t,$$
$$\mathbf{x}(\boldsymbol{\xi}, t) = \mathcal{A}_t(\boldsymbol{\xi})$$

domain velocity
$$\mathbf{w}(\mathbf{x}, t) = \frac{\partial \mathcal{A}_t}{\partial t} \circ \mathcal{A}_t^{-1}(\mathbf{x})$$

ALE derivative
$$\left.\frac{\partial \mathbf{u}}{\partial t}\right|_{\boldsymbol{\xi}} = \left.\frac{\partial \mathbf{u}}{\partial t}\right|_{\mathbf{x}} + \mathbf{w} \cdot \nabla_{\mathbf{x}} \mathbf{u}$$

ALE Formulation

- The moving domain is recast at each time t to a fixed configuration Ω_0^f through the ALE mapping $\mathcal{A}_t$:

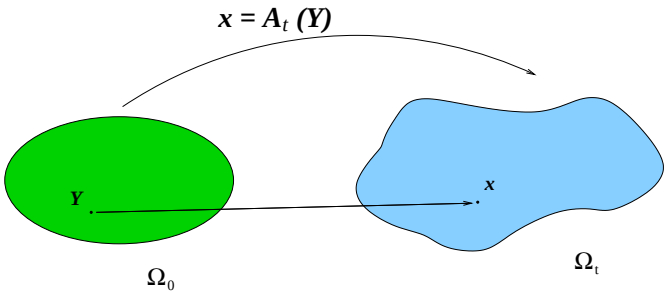

$$\mathcal{A}_t : \Omega_0 \longrightarrow \Omega_t,$$
$$\mathbf{x}(\boldsymbol{\xi}, t) = \mathcal{A}_t(\boldsymbol{\xi})$$

Navier-Stokes ALE

$$\begin{cases} \varrho_f \left.\dfrac{\partial \mathbf{u}}{\partial t}\right|_{\boldsymbol{\xi}} + \varrho_f(\mathbf{u} - \mathbf{w}\cdot\nabla)\mathbf{u} - \operatorname{div}\boldsymbol{\sigma}_\mathbf{f}(\mathbf{u}, p) = \mathbf{0} \\ \operatorname{div}\mathbf{u} = 0 \end{cases} \quad \text{in } \Omega_t$$

Finite Element ALE approximation

- We introduce a mesh $\mathcal{T}_{h0}$ in the reference domain. The ALE mapping induces a mesh $\mathcal{T}_{ht}$ in Ω_t at each time t.
- Given the deformation of the boundary, the ALE mapping can be built by interpolation or solution of a differential problem (e.g. harmonic extension of the boundary displacement)
- The unknowns are associated to the nodes of $\mathcal{T}_{ht}$, which move in time.
- The ALE derivative is the derivative of the unknowns along the trajectories of the nodes; it can be easily discretized
- The discretization of the spatial operators is done on the current configuration Ω_t (much easier).

Finite Element ALE approximation

- We introduce a mesh $\mathcal{T}_{h0}$ in the reference domain. The ALE mapping induces a mesh $\mathcal{T}_{ht}$ in Ω_t at each time t.
- Given the deformation of the boundary, the ALE mapping can be built by interpolation or solution of a differential problem (e.g. harmonic extension of the boundary displacement)
- The unknowns are associated to the nodes of $\mathcal{T}_{ht}$, which move in time.
- The ALE derivative is the derivative of the unknowns along the trajectories of the nodes; it can be easily discretized
- The discretization of the spatial operators is done on the current configuration Ω_t (much easier).

Finite Element ALE approximation

- We introduce a mesh $\mathcal{T}_{h0}$ in the reference domain. The ALE mapping induces a mesh $\mathcal{T}_{ht}$ in Ω_t at each time t.
- Given the deformation of the boundary, the ALE mapping can be built by interpolation or solution of a differential problem (e.g. harmonic extension of the boundary displacement)
- The unknowns are associated to the nodes of $\mathcal{T}_{ht}$, which move in time.
- The ALE derivative is the derivative of the unknowns along the trajectories of the nodes; it can be easily discretized
- The discretization of the spatial operators is done on the current configuration Ω_t (much easier).

Finite Element ALE approximation

- We introduce a mesh $\mathcal{T}_{h0}$ in the reference domain. The ALE mapping induces a mesh $\mathcal{T}_{ht}$ in Ω_t at each time t.
- Given the deformation of the boundary, the ALE mapping can be built by interpolation or solution of a differential problem (e.g. harmonic extension of the boundary displacement)
- The unknowns are associated to the nodes of $\mathcal{T}_{ht}$, which move in time.
- The ALE derivative is the derivative of the unknowns along the trajectories of the nodes; it can be easily discretized
- The discretization of the spatial operators is done on the current configuration Ω_t (much easier).

Finite Element ALE approximation

- We introduce a mesh $\mathcal{T}_{h0}$ in the reference domain. The ALE mapping induces a mesh $\mathcal{T}_{ht}$ in Ω_t at each time t.
- Given the deformation of the boundary, the ALE mapping can be built by interpolation or solution of a differential problem (e.g. harmonic extension of the boundary displacement)
- The unknowns are associated to the nodes of $\mathcal{T}_{ht}$, which move in time.
- The ALE derivative is the derivative of the unknowns along the trajectories of the nodes; it can be easily discretized
- The discretization of the spatial operators is done on the current configuration Ω_t (much easier).

Partitioned algorithms

- The fluid-structure coupled system is highly non linear since the fluid domain Ω_t^f, the ALE mapping $\mathcal{A}_t$ and the domain velocity **w** all depend on the unknown displacement η. A direct solution of the global non-linear system (monolithic approach) is very costly.

- Partitioned time marching algorithms are based on subsequent solutions of fluid and structure subproblems
  - allow one to reuse existing computational codes.
  - each subproblem can be solved with the most efficient available numerical algorithms (e.g. projection schemes for Navier-Stokes, updated Lagrangian for structure dynamics, ...)

Partitioned algorithms

•The fluid-structure coupled system is highly non linear since the fluid domain Ω_t^f, the ALE mapping $\mathcal{A}_t$ and the domain velocity **w** all depend on the unknown displacement η. A direct solution of the global non-linear system (monolithic approach) is very costly.

•Partitioned time marching algorithms are based on subsequent solutions of fluid and structure subproblems

- allow one to reuse existing computational codes.
- each subproblem can be solved with the most efficient available numerical algorithms (e.g. projection schemes for Navier-Stokes, updated Lagrangian for structure dynamics, ...)

Explicit partitioned algorithms
also called "loosely coupled" or "staggered"

In each time step solve only once (or just a few times) the fluid and structure problems

Example

1. Solve structure pb. with Neumann b.cs ($\eta^n = \eta^n(\boldsymbol{\sigma}_f(\mathbf{u}^{n-1}, p^{n-1}))$)
2. Update fluid mesh ($\mathcal{A}_{t^n} = \mathcal{A}_{t^n}(\eta^n)$)
3. Solve fluid pb. with Dirichelet b.cs (compute $(\mathbf{u}^n, p^n)$)
4. go to next time step

- Typically obtained by combining an explicit discretization for the structure and an implicit discr. for the fluid.
- The continuity of the stresses at the interface is not satisfied exactly.
  $\Rightarrow$ Energy is not perfectly balanced.
- A predictor corrector strategy can be added to the algorithm [see C. Farhat, S. Piperno, ...] to reduce the "energy error"

Explicit partitioned algorithms
also called "loosely coupled" or "staggered"

In each time step solve only once (or just a few times) the fluid and structure problems

Example

1. Solve structure pb. with Neumann b.cs ($\eta^n = \eta^n(\boldsymbol{\sigma}_f(\mathbf{u}^{n-1}, p^{n-1}))$)
2. Update fluid mesh ($\mathcal{A}_{t^n} = \mathcal{A}_{t^n}(\eta^n)$)
3. Solve fluid pb. with Dirichelet b.cs (compute $(\mathbf{u}^n, p^n)$)
4. go to next time step

- Typically obtained by combining an explicit discretization for the structure and an implicit discr. for the fluid.
- The continuity of the stresses at the interface is not satisfied exactly.
  $\Rightarrow$ Energy is not perfectly balanced.
- A predictor corrector strategy can be added to the algorithm [see C. Farhat, S. Piperno, ...] to reduce the "energy error"

Explicit partitioned algorithms
also called "loosely coupled" or "staggered"

In each time step solve only once (or just a few times) the fluid and structure problems

Example

1. Solve structure pb. with Neumann b.cs ($\eta^n = \eta^n(\boldsymbol{\sigma}_f(\mathbf{u}^{n-1}, p^{n-1}))$)
2. Update fluid mesh ($\mathcal{A}_{t^n} = \mathcal{A}_{t^n}(\eta^n)$)
3. Solve fluid pb. with Dirichelet b.cs (compute $(\mathbf{u}^n, p^n)$)
4. go to next time step

- Typically obtained by combining an explicit discretization for the structure and an implicit discr. for the fluid.
- The continuity of the stresses at the interface is not satisfied exactly.
  $\Rightarrow$ Energy is not perfectly balanced.
- A predictor corrector strategy can be added to the algorithm [see C. Farhat, S. Piperno, ...] to reduce the "energy error"

Explicit partitioned algorithms
also called "loosely coupled" or "staggered"

In each time step solve only once (or just a few times) the fluid and structure problems

Example

1. Solve structure pb. with Neumann b.cs ($\eta^n = \eta^n(\boldsymbol{\sigma}_f(\mathbf{u}^{n-1}, p^{n-1}))$)
2. Update fluid mesh ($\mathcal{A}_{t^n} = \mathcal{A}_{t^n}(\eta^n)$)
3. Solve fluid pb. with Dirichelet b.cs (compute $(\mathbf{u}^n, p^n)$)
4. go to next time step

- Typically obtained by combining an explicit discretization for the structure and an implicit discr. for the fluid.
- The continuity of the stresses at the interface is not satisfied exactly.
  $\Rightarrow$ Energy is not perfectly balanced.
- A predictor corrector strategy can be added to the algorithm [see C. Farhat, S. Piperno, ...] to reduce the "energy error"

Implicit partitioned algorithms

- At each time step enforce exactly both coupling conditions at the interface (Energy balanced)
- All the equations are coupled in each time step $\Longrightarrow$ need subiterations

Example: Fixed point (or Dirichlet Neumann) iterations

In each time step $[t^n, t^{n+1}]$, and $\forall k > 0$ solve

1. Solve structure pb. with Neumann b.cs $(\eta_k = \eta_k(\boldsymbol{\sigma}_f(\mathbf{u}_{k-1}, p_{k-1})))$
2. Update fluid mesh $(\mathcal{A}_k = \mathcal{A}_k(\eta^k))$
3. Solve fluid pb. with Dirichlet b.cs (compute $(\mathbf{u}_k, p_k)$)
4. Recompute structure $(\eta_{k+1} = \eta_{k+1}(\boldsymbol{\sigma}_\mathbf{f}(\mathbf{u_k}, \mathbf{p_k})))$
5. **if** $\|\eta_{k+1} - \eta_k\| < tol$ **then** go to next time step
   else relax the solution η_{k+1} and go to 2.

Implicit partitioned algorithms

- At each time step enforce exactly both coupling conditions at the interface (Energy balanced)
- All the equations are coupled in each time step $\Longrightarrow$ need subiterations

Example: Fixed point (or Dirichlet Neumann) iterations

In each time step $[t^n, t^{n+1}]$, and $\forall k > 0$ solve

1. Solve structure pb. with Neumann b.cs $(\eta_k = \eta_k(\boldsymbol{\sigma}_f(\mathbf{u}_{k-1}, p_{k-1})))$
2. Update fluid mesh $(\mathcal{A}_k = \mathcal{A}_k(\eta^k))$
3. Solve fluid pb. with Dirichlet b.cs (compute $(\mathbf{u}_k, p_k)$)
4. Recompute structure $(\eta_{k+1} = \eta_{k+1}(\boldsymbol{\sigma}_\mathbf{f}(\mathbf{u_k}, \mathbf{p_k})))$
5. **if** $\|\eta_{k+1} - \eta_k\| < tol$ **then** go to next time step
   else relax the solution η_{k+1} and go to 2.

Implicit partitioned algorithms

•At each time step enforce exactly both coupling conditions at the interface (Energy balanced)

•All the equations are coupled in each time step $\Longrightarrow$ need subiterations

Example: Fixed point (or Dirichlet Neumann) iterations

In each time step $[t^n, t^{n+1}]$, and $\forall k > 0$ solve

1. Solve structure pb. with Neumann b.cs $(\eta_k = \eta_k(\boldsymbol{\sigma}_f(\mathbf{u}_{k-1}, p_{k-1})))$
2. Update fluid mesh $(\mathcal{A}_k = \mathcal{A}_k(\eta^k))$
3. Solve fluid pb. with Dirichlet b.cs (compute $(\mathbf{u}_k, p_k)$)
4. Recompute structure $(\eta_{k+1} = \eta_{k+1}(\boldsymbol{\sigma}_\mathbf{f}(\mathbf{u_k}, \mathbf{p_k})))$
5. **if** $\|\eta_{k+1} - \eta_k\| < tol$ **then** go to next time step
   else relax the solution η_{k+1} and go to 2.

Numerical observations

In haemodymanics applications (thin structure in cylindrical configuration) **numerical tests** [Nobile, Ph.D] show that explicit algorithms become unstable when

- $\varrho_s^0 h_s / \varrho_f$ small
- L/D large (L=length, D=diameter of the tube)

irrespectively of the time step chosen!!!

- Under the same conditions, implicit Block Gauss-Seidel iterative algorithms need very small relaxation parameters to converge.

Numerical observations

In haemodymanics applications (thin structure in cylindrical configuration) **numerical tests** [Nobile, Ph.D] show that explicit algorithms become unstable when

- $\varrho_s^0 h_s / \varrho_f$ small
- L/D large (L=length, D=diameter of the tube)

irrespectively of the time step chosen!!!

•Under the same conditions, implicit Block Gauss-Seidel iterative algorithms need very small relaxation parameters to converge.

How to get stable implicit schemes: example IE+BDF

•Let us start from the global weak (ALE) formulation and consider as time discretization: Implicit Euler (fluid) and BDF1 (structure)

$$\varrho_f \frac{d}{dt} \int_{\Omega^f(t)} (\mathbf{u} + \mathrm{div}(\mathbf{u} \otimes (\mathbf{u} - \mathbf{w}))) \cdot \mathbf{v} + \boldsymbol{\sigma}_f(\mathbf{u}, p) : \nabla \mathbf{v} + \mathrm{div}\, \mathbf{u} q +$$

$$\int_{\Omega_0^s} \varrho_s^0 \frac{\partial^2 \boldsymbol{\eta}}{\partial t^2} \cdot \boldsymbol{\phi} + \mathbf{F}(\boldsymbol{\eta})\mathbf{S}(\boldsymbol{\eta}) : \nabla_0 \boldsymbol{\phi} = \int_{\Omega_t^f} \mathbf{f}^f \cdot \mathbf{v} + \int_{\Omega_0^s} f_0^s \cdot \boldsymbol{\phi}$$

+ coupling condition $\mathbf{u}^n \circ \mathbf{x}(\boldsymbol{\xi}) = \frac{\partial \boldsymbol{\eta}}{\partial t}$

How to get stable implicit schemes: example IE+BDF

•Let us start from the global weak (ALE) formulation and consider as time discretization: Implicit Euler (fluid) and BDF1 (structure)

$$\frac{\varrho_f}{\Delta t}\int_{\Omega^f(t^n)}\mathbf{u}^n\cdot\mathbf{v}-\frac{\varrho_f}{\Delta t}\int_{\Omega^f(t^{n-1})}\mathbf{u}^{n-1}\cdot\mathbf{v}+\int_{\Omega^f(t^n)}\varrho_f\,\mathrm{div}(\mathbf{u}^n\otimes(\mathbf{u}^n-\mathbf{w}^n))\cdot\mathbf{v}+$$

$$\int_{\Omega^f(t^n)}\boldsymbol{\sigma}_f(\mathbf{u}^n,p^n):\nabla\mathbf{v}+\mathrm{div}\,\mathbf{u}^n q+\int_{\Omega_0^s}\varrho_s^0\frac{\boldsymbol{\eta}^n-2\boldsymbol{\eta}^{n-1}+\boldsymbol{\eta}^{n-2}}{\Delta t^2}\cdot\boldsymbol{\phi}+$$

$$\mathbf{F}(\boldsymbol{\eta}^n)\mathbf{S}(\boldsymbol{\eta}^n):\nabla_0\boldsymbol{\phi}=\int_{\Omega^f(t^n)}\mathbf{f}^f(t^n)\cdot\mathbf{v}+\int_{\Omega_0^s}f_0^s(t^n)\cdot\boldsymbol{\phi}$$

+ coupling condition $\mathbf{u}^n\circ\mathbf{x}(\boldsymbol{\xi})=\frac{\boldsymbol{\eta}^n-\boldsymbol{\eta}^{n-1}}{\Delta t}$

How to get stable implicit schemes: example IE+BDF

- To get global stability, the ALE-convective term has to be integrated on intermediate configurations so as to satisfy the so called Geometric Conservation Laws (GCL) [Formaggia-Nobile, '99, '04]

Stability Result for homogeneous problem [Nobile, PhD]

$$\frac{\varrho_f}{2}\|\mathbf{u}^n\|^2_{L^2(\Omega^f(t^n))} + \frac{\varrho_0^s}{2}\|\frac{\boldsymbol{\eta}^n - \boldsymbol{\eta}^{n-1}}{\Delta t}\|^2_{L^2(\Omega_0^s)} + \int_{\Omega_0^s} W(\boldsymbol{\eta}^n)\, d\Omega$$
$$+ \sum_i \Delta t \int_{\Omega^f(t^i)} \mathbf{D}(\mathbf{u}^i) : \mathbf{D}(\mathbf{u}^i)\, d\Omega$$
$$\leq \frac{\varrho_f}{2}\|\mathbf{u}^0\|^2_{L^2(\Omega_0^f)} + \frac{\varrho_0^s}{2}\|\dot{\boldsymbol{\eta}}^0\|^2_{L^2(\Omega_0^s)} + \int_{\Omega_0^s} W(0)\, d\Omega$$

Mathematical explanation of instabilities

We consider an over-simplified model:

- Fluid model: potential flow (no viscous and convective terms; only the incompressibility of the fluid is kept)
- Fluid geometry is kept fixed
- Independent rings model for the structure

- This model features the same numerical instabilities as the more complex (and non-linear) one.

Conclusions: the source of the instability is the *incompressibility of the fluid*

Mathematical explanation of instabilities

We consider an over-simplified model:

- Fluid model: potential flow (no viscous and convective terms; only the incompressibility of the fluid is kept)
- Fluid geometry is kept fixed
- Independent rings model for the structure

•This model features the same numerical instabilities as the more complex (and non-linear) one.

Conclusions: the source of the instability is the *incompressibility of the fluid*

Mathematical explanation of instabilities

We consider an over-simplified model:

- Fluid model: potential flow (no viscous and convective terms; only the incompressibility of the fluid is kept)
- Fluid geometry is kept fixed
- Independent rings model for the structure

•This model features the same numerical instabilities as the more complex (and non-linear) one.

Conclusions: the source of the instability is the *incompressibility of the fluid*

Simple FSI model

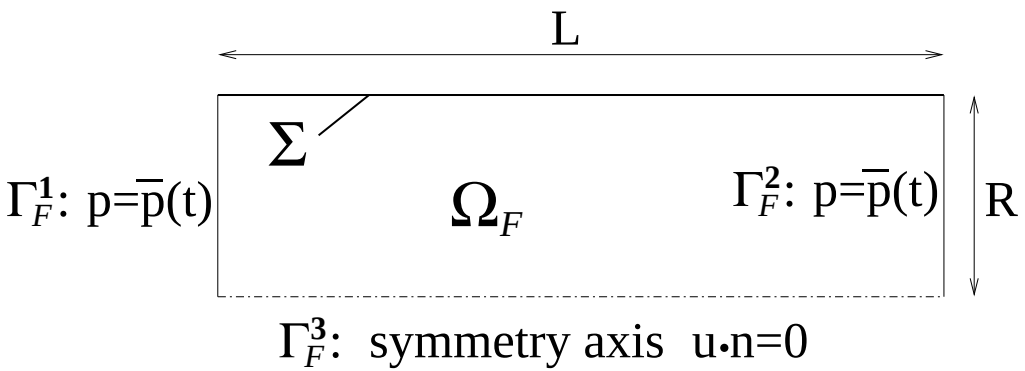

Structure $\rho_w h_s \partial_{tt}^2 \eta - a \partial_{xx}^2 \eta + b\eta = p$ on Σ

Fluid
$$\begin{cases} \rho_f \partial_t \mathbf{u} + \nabla p = 0 \quad \text{on } \Omega_F \\ \operatorname{div} \mathbf{u} = 0 \\ \mathbf{u} \cdot \mathbf{n} = \partial_t \eta \ \text{ on } \Sigma \\ + \ b.c. \end{cases}$$

$\xrightarrow{\text{div}}$

$$\begin{cases} \Delta p = 0 \\ \partial_{\mathbf{n}} p = -\rho_f \partial_{tt}^2 \eta \\ + \ b.c. \end{cases}$$

Simple FSI model

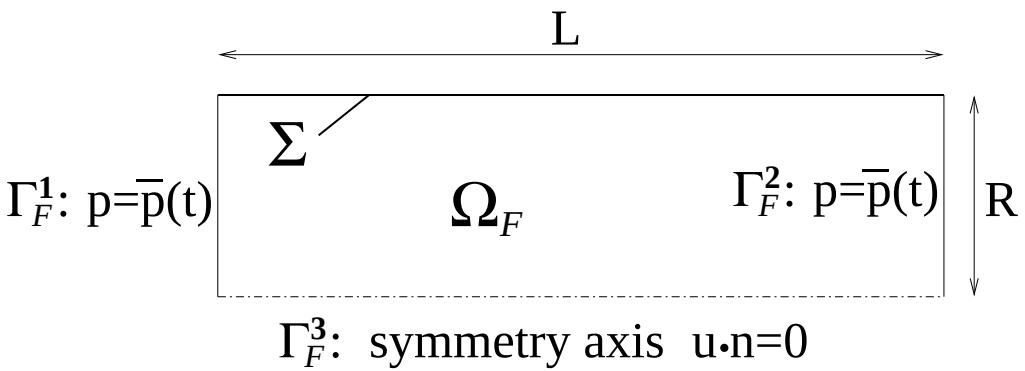

Structure $\rho_w h_s \partial_{tt}^2 \eta - a \partial_{xx}^2 \eta + b\eta = p$ on Σ

Fluid
$$\begin{cases} \rho_f \partial_t \mathbf{u} + \nabla p = 0 \quad \text{on } \Omega_F \\ \operatorname{div} \mathbf{u} = 0 \\ \mathbf{u} \cdot \mathbf{n} = \partial_t \eta \ \text{ on } \Sigma \\ + \ b.c. \end{cases} \xrightarrow{\text{div}} \begin{cases} \Delta p = 0 \\ \partial_{\mathbf{n}} p = -\rho_f \partial_{tt}^2 \eta \\ + \ b.c. \end{cases}$$

Functional setting

For any $w \in H^{-1/2}(\Sigma)$, we denote by $\mathcal{R}w$ solution to the following problem

$$\begin{cases} -\Delta \mathcal{R}w = 0 & \text{in } \Omega_F, \\ \dfrac{\partial \mathcal{R}w}{\partial n} = w & \text{on } \Sigma \\ + \text{ homogeneous b.c.} & \text{on } \Gamma_F^1, \Gamma_F^2, \Gamma_F^3 \end{cases}$$

Added mass operator: (inverse of Steklov-Poincaré)

$$\mathcal{M}_{\mathcal{A}} : H^{-1/2}(\Sigma) \to H^{1/2}(\Sigma), \qquad \mathcal{M}_{\mathcal{A}} w = \mathcal{R}w|_{\Sigma}.$$

- The operator $\mathcal{M}_{\mathcal{A}}$ is continuous on $H^{1/2}(\Sigma)$ and compact, self-adjoint and positive on $L^2(\Sigma)$.

Functional setting

For any $w \in H^{-1/2}(\Sigma)$, we denote by $\mathcal{R}w$ solution to the following problem

$$\begin{cases} -\Delta \mathcal{R}w = 0 & \text{in } \Omega_F, \\ \dfrac{\partial \mathcal{R}w}{\partial n} = w & \text{on } \Sigma \\ + \text{ homogeneous b.c.} & \text{on } \Gamma_F^1, \Gamma_F^2, \Gamma_F^3 \end{cases}$$

Added mass operator: (inverse of Steklov-Poincaré)

$$\mathcal{M}_{\mathcal{A}} : H^{-1/2}(\Sigma) \to H^{1/2}(\Sigma), \qquad \mathcal{M}_{\mathcal{A}} w = \mathcal{R}w|_{\Sigma}.$$

- The operator $\mathcal{M}_{\mathcal{A}}$ is continuous on $H^{1/2}(\Sigma)$ and compact, self-adjoint and positive on $L^2(\Sigma)$.

Functional setting – cont.

We also introduce the particular solution p^* to the problem with non-homogeneous boundary conditions:

$$\begin{cases} -\Delta p^* = 0 & \text{in } \Omega_F, \\ \frac{\partial p^*}{\partial n} = 0 & \text{on } \Gamma_F^3 \cup \Sigma, \\ p^* = \bar{p} & \text{on } \Gamma_F^1 \cup \Gamma_F^2 \end{cases}$$

We have that $p = p^* - \rho_f \mathcal{R} \frac{\partial^2 \eta}{\partial t^2}$.

and, setting $p_{ext} = p^*|_\Sigma$

$$p|_\Sigma = p_{ext} - \rho_f \mathcal{M}_\mathcal{A} \frac{\partial^2 \eta}{\partial t^2}$$

Added-mass equation

Substituting the previous expression in the structure equation we get

$$(\rho_s h_s \mathcal{I} + \rho_f \mathcal{M}_{\mathcal{A}}) \frac{\partial^2 \eta}{\partial t^2} - a \frac{\partial^2 \eta}{\partial x^2} + b\eta = p_{ext} \qquad (*)$$

- Equation (*) is similar to the structure equation except for the extra term $\rho_f \mathcal{M}_{\mathcal{A}}$.
- This operator represents the interaction of the fluid on the structure and acts as an extra mass ($\rightarrow$ "added-mass" effect).
- Problem (*) admits a unique solution $\eta \in \mathcal{C}([0, \infty), H^1(\Sigma))$.

Added-mass equation

Substituting the previous expression in the structure equation we get

$$(\rho_s h_s \mathcal{I} + \rho_f \mathcal{M}_{\mathcal{A}}) \frac{\partial^2 \eta}{\partial t^2} - a \frac{\partial^2 \eta}{\partial x^2} + b\eta = p_{ext} \qquad (*)$$

- Equation (*) is similar to the structure equation except for the extra term $\rho_f \mathcal{M}_{\mathcal{A}}$.
- This operator represents the interaction of the fluid on the structure and acts as an extra mass ($\rightarrow$ "added-mass" effect).
- Problem (*) admits a unique solution $\eta \in \mathcal{C}([0, \infty), H^1(\Sigma))$.

Added-mass equation

Substituting the previous expression in the structure equation we get

$$(\rho_s h_s \mathcal{I} + \rho_f \mathcal{M}_{\mathcal{A}}) \frac{\partial^2 \eta}{\partial t^2} - a \frac{\partial^2 \eta}{\partial x^2} + b\eta = p_{ext} \qquad (*)$$

- Equation (*) is similar to the structure equation except for the extra term $\rho_f \mathcal{M}_{\mathcal{A}}$.
- This operator represents the interaction of the fluid on the structure and acts as an extra mass ($\rightarrow$ "added-mass" effect).
- Problem (*) admits a unique solution $\eta \in \mathcal{C}([0, \infty), H^1(\Sigma))$.

Added-mass equation

Substituting the previous expression in the structure equation we get

$$(\rho_s h_s \mathcal{I} + \rho_f \mathcal{M}_\mathcal{A}) \frac{\partial^2 \eta}{\partial t^2} - a \frac{\partial^2 \eta}{\partial x^2} + b\eta = p_{ext} \qquad (*)$$

- Equation (*) is similar to the structure equation except for the extra term $\rho_f \mathcal{M}_\mathcal{A}$.
- This operator represents the interaction of the fluid on the structure and acts as an extra mass ($\rightarrow$ "added-mass" effect).
- Problem (*) admits a unique solution $\eta \in \mathcal{C}([0,\infty), H^1(\Sigma))$.

Spectrum of the added-mass operator

It is useful to study the behaviour of the maximum eigenvalue μ_{max} of $\mathcal{M}_\mathcal{A}$

- The inverse of μ_{max} is the smallest eigenvalue of the standard Steklov-Poincaré operator.
- μ_{max} is a purely geometric quantity.

It can be computed analytically in simple cases:

•2D fluid in rectangle: $\mu_{max} = \frac{L}{\pi \text{th}\left(\frac{\pi R}{L}\right)}$.

•2D axi-symmetric fluid in cylinder $\mu_{max} = \frac{L I_0\left(\frac{\pi R}{L}\right)}{\pi I_0'\left(\frac{\pi R}{L}\right)}$ where I_0 is the modified Bessel function. For R/L small, $\mu_{max} \approx \frac{2L^2}{\pi^2 R}$.

Spectrum of the added-mass operator

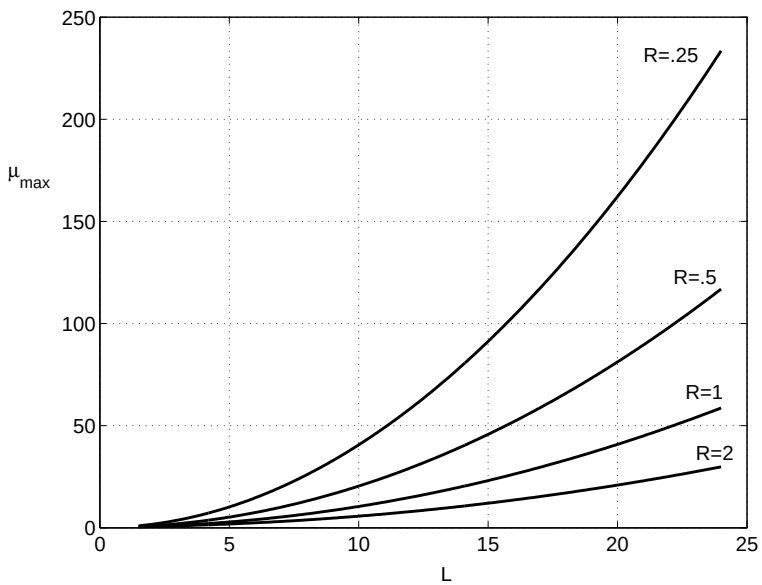

μ_{max} in the 2D case

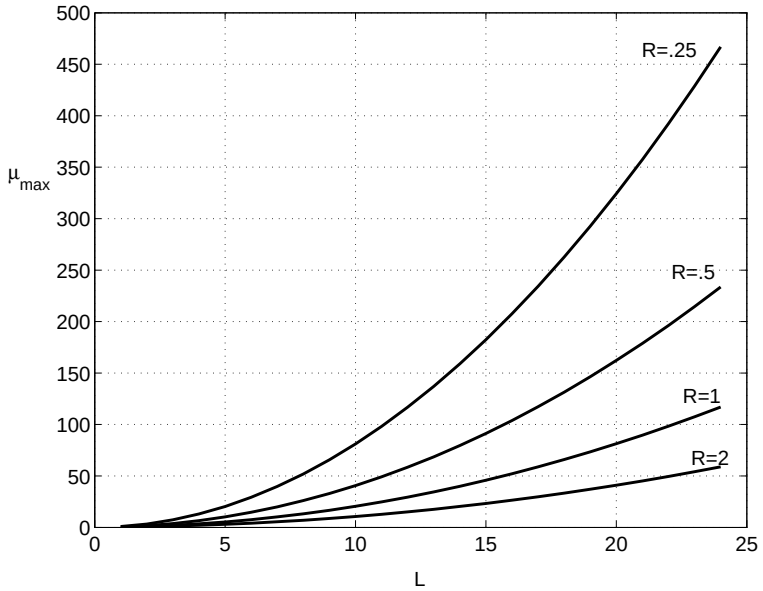

μ_{max} in the 2D axisymm. case

Instability of explicit algorithms

Prototype of explicit algorithm: Leap-frog for the structure and Implicit Euler for the fluid (LF-IE).

$$\begin{cases} \rho_f \dfrac{\mathbf{u}^n - \mathbf{u}^{n-1}}{\Delta t} + \nabla p^n = 0 \\ \operatorname{div} \mathbf{u}^n = 0 \\ \mathbf{u}^n = \dfrac{\eta^n - \eta^{n-1}}{\Delta t}\,\mathbf{n} \end{cases} \xrightarrow{\text{div}} \begin{cases} \Delta p^n = 0 \\ \partial_{\mathbf{n}} p^n = -\rho_f \dfrac{\eta^n - 2\eta^{n-1} + \eta^{n-2}}{\Delta t^2} \end{cases}$$

$$\rho_w h_s \frac{\eta^{n+1} - 2\eta^n + \eta^{n-1}}{\Delta t^2} + b\eta^n = p^n + p^n_{ext} \qquad \text{on } \Sigma$$

Instability of explicit algorithms

Prototype of explicit algorithm: Leap-frog for the structure and Implicit Euler for the fluid (LF-IE).

$$\begin{cases} \rho_f \dfrac{\mathbf{u}^n - \mathbf{u}^{n-1}}{\Delta t} + \nabla p^n = 0 \\ \operatorname{div} \mathbf{u}^n = 0 \\ \mathbf{u}^n = \dfrac{\eta^n - \eta^{n-1}}{\Delta t}\,\mathbf{n} \end{cases} \xrightarrow{\text{div}} \begin{cases} \Delta p^n = 0 \\ \partial_{\mathbf{n}} p^n = -\rho_f \dfrac{\eta^n - 2\eta^{n-1} + \eta^{n-2}}{\Delta t^2} \end{cases}$$

$$\rho_w h_s \frac{\eta^{n+1} - 2\eta^n + \eta^{n-1}}{\Delta t^2} + b\eta^n = p^n + p^n_{ext} \qquad \text{on } \Sigma$$

This algorithm is equivalent to the 3 steps difference eq.

$$\rho_w h_s \frac{\eta^{n+1} - 2\eta^n + \eta^{n-1}}{\Delta t^2} + b\eta^n = -\rho_f \mathcal{M}_{\mathcal{A}} \frac{\eta^n - 2\eta^{n-1} + \eta^{n-2}}{\Delta t^2} + p^n_{ext}$$

Proposition 1 [Causin, Gerbeau, Nobile 2004]

The explicit *Leap-Frog/Implicit Euler* algorithm is unconditionally unstable if

$$\frac{\varrho_s h_s}{\rho_f \mu_{max}} < 1$$

- the scheme is unstable when $\varrho_s h_s / \varrho_f$ small or μ_{max} large.

This algorithm is equivalent to the 3 steps difference eq.

$$\rho_w h_s \frac{\eta^{n+1} - 2\eta^n + \eta^{n-1}}{\Delta t^2} + b\eta^n = -\rho_f \mathcal{M}_{\mathcal{A}} \frac{\eta^n - 2\eta^{n-1} + \eta^{n-2}}{\Delta t^2} + p^n_{ext}$$

Proposition 1 [Causin, Gerbeau, Nobile 2004]

The explicit *Leap-Frog/Implicit Euler* algorithm is unconditionally unstable if

$$\frac{\varrho_s h_s}{\rho_f \mu_{max}} < 1$$

- the scheme is unstable when $\varrho_s h_s / \varrho_f$ small or μ_{max} large.

This algorithm is equivalent to the 3 steps difference eq.

$$\rho_w h_s \frac{\eta^{n+1} - 2\eta^n + \eta^{n-1}}{\Delta t^2} + b\eta^n = -\rho_f \mathcal{M}_{\mathcal{A}} \frac{\eta^n - 2\eta^{n-1} + \eta^{n-2}}{\Delta t^2} + p^n_{ext}$$

Proposition 1 [Causin, Gerbeau, Nobile 2004]

The explicit *Leap-Frog/Implicit Euler* algorithm is unconditionally unstable if

$$\frac{\varrho_s h_s}{\rho_f \mu_{max}} < 1$$

- the scheme is unstable when $\varrho_s h_s / \varrho_f$ small or μ_{max} large.

Sketch of the Proof. Expand η and p_{ext} on the basis of eigenvectors of $\mathcal{M}_{\mathcal{A}}$. For each component, the characteristic polynomial $\chi(s) \in \mathbb{P}^3$ of the 3 step difference equation is s.t.

$$\chi(-\infty) = -\infty, \qquad \chi(-1) = b + 4(\rho_f \mu_i - \rho_w h)/\Delta t^2$$

Hence, if $\varrho_f \mu_{max} \geq \varrho_s h_s$, then

$$\chi(-1) \geq 0 \qquad \Longrightarrow \qquad \exists s^* \leq -1 \text{ s.t. } \chi(s^*) = 0, \qquad \forall \Delta t!!!!$$

Implicit algorithms

Prototype of implicit algorithm: Implicit Euler for the fluid and first order BDF for the structure (BDF+IE)

$$\begin{cases} \rho_f \dfrac{\mathbf{u}^{n+1} - \mathbf{u}^n}{\Delta t} + \nabla p^{n+1} = 0 \\ \operatorname{div} \mathbf{u}^{n+1} = 0 \\ \mathbf{u}^{n+1} = \dfrac{\eta^{n+1} - \eta^n}{\Delta t}\,\mathbf{n} \end{cases} \xrightarrow{\text{div}} \begin{cases} \Delta p^{n+1} = 0 \\ \partial_{\mathbf{n}} p^{n+1} = -\rho_f \dfrac{\eta^{n+1} - 2\eta^n + \eta^{n-1}}{\Delta t^2} \end{cases}$$

$$\rho_w h_s \frac{\eta^{n+1} - 2\eta^n + \eta^{n-1}}{\Delta t^2} + b\eta^{n+1} = p^{n+1} + p_{ext}^{n+1} \qquad \text{on } \Sigma$$

Implicit algorithms

Prototype of implicit algorithm: Implicit Euler for the fluid and first order BDF for the structure (BDF+IE)

$$\begin{cases} \rho_f \dfrac{\mathbf{u}^{n+1}-\mathbf{u}^n}{\Delta t} + \nabla p^{n+1} = 0 \\ \operatorname{div} \mathbf{u}^{n+1} = 0 \\ \mathbf{u}^{n+1} = \dfrac{\eta^{n+1}-\eta^n}{\Delta t}\,\mathbf{n} \end{cases} \xrightarrow{\text{div}} \begin{cases} \Delta p^{n+1} = 0 \\ \partial_{\mathbf{n}} p^{n+1} = -\rho_f \dfrac{\eta^{n+1}-2\eta^n+\eta^{n-1}}{\Delta t^2} \end{cases}$$

$$\rho_w h_s \frac{\eta^{n+1}-2\eta^n+\eta^{n-1}}{\Delta t^2} + b\eta^{n+1} = p^{n+1} + p_{ext}^{n+1} \qquad \text{on } \Sigma$$

equivalent to the 2 step difference equation

$$(\rho_w h_s \mathcal{I} + \rho_f \mathcal{M}_\mathcal{A}) \frac{\eta^{n+1} - 2\eta^n + \eta^{n-1}}{\Delta t^2} + b\eta^{n+1} = p_{ext}^{n+1}$$

- Stable discretization for any Δt.
- Implicit discretization $\longrightarrow$ need subiterations.

Partitioned algorithms: let's consider the two strategies

- Dirichlet/Neumann (D-N): at each iteration solve the fluid with imposed velocity at the interface and the structure with imposed loads.
- Neumann/Dirichlet (N-D): solve the fluid equations subjected to the structure load and update structure displacement.

equivalent to the 2 step difference equation

$$(\rho_w h_s \mathcal{I} + \rho_f \mathcal{M}_\mathcal{A}) \frac{\eta^{n+1} - 2\eta^n + \eta^{n-1}}{\Delta t^2} + b\eta^{n+1} = p_{ext}^{n+1}$$

- Stable discretization for any Δt.
- Implicit discretization $\longrightarrow$ need subiterations.

Partitioned algorithms: let's consider the two strategies

- Dirichlet/Neumann (D-N): at each iteration solve the fluid with imposed velocity at the interface and the structure with imposed loads.
- Neumann/Dirichlet (N-D): solve the fluid equations subjected to the structure load and update structure displacement.

equivalent to the 2 step difference equation

$$(\rho_w h_s \mathcal{I} + \rho_f \mathcal{M}_\mathcal{A}) \frac{\eta^{n+1} - 2\eta^n + \eta^{n-1}}{\Delta t^2} + b\eta^{n+1} = p_{ext}^{n+1}$$

- Stable discretization for any Δt.
- Implicit discretization $\longrightarrow$ need subiterations.

Partitioned algorithms: let's consider the two strategies

- Dirichlet/Neumann (D-N): at each iteration solve the fluid with imposed velocity at the interface and the structure with imposed loads.
- Neumann/Dirichlet (N-D): solve the fluid equations subjected to the structure load and update structure displacement.

equivalent to the 2 step difference equation

$$(\rho_w h_s \mathcal{I} + \rho_f \mathcal{M}_\mathcal{A}) \frac{\eta^{n+1} - 2\eta^n + \eta^{n-1}}{\Delta t^2} + b\eta^{n+1} = p_{ext}^{n+1}$$

- Stable discretization for any Δt.
- Implicit discretization $\longrightarrow$ need subiterations.

Partitioned algorithms: let's consider the two strategies

- Dirichlet/Neumann (D-N): at each iteration solve the fluid with imposed velocity at the interface and the structure with imposed loads.
- Neumann/Dirichlet (N-D): solve the fluid equations subjected to the structure load and update structure displacement.

Dirichlet-Neumann method

given an initial guess η_0^{n+1}, *we solve for each* $k = 1, 2, \ldots$

i. $\Delta p_k = 0$ in Ω_F

$\partial_{\mathbf{n}} p_k = -\rho_f \dfrac{\eta_{k-1} - 2\eta^n + \eta^{n-1}}{\Delta t^2}$ on Σ

ii. $\rho_w h_s \dfrac{\tilde{\eta}_k - 2\eta^n + \eta^{n-1}}{\Delta t^2} + b\tilde{\eta}_k = p_k + p_{ext}^{n+1}$ on Σ

iii. $\eta_k = \omega\tilde{\eta}_k + (1-\omega)\eta_{k-1}$

- equivalent to a fixed point algorithm on η^{n+1}.

Dirichlet-Neumann method

given an initial guess η_0^{n+1}, *we solve for each* $k = 1, 2, \ldots$

i. $\Delta p_k = 0$ in Ω_F

$\partial_{\mathbf{n}} p_k = -\rho_f \dfrac{\eta_{k-1} - 2\eta^n + \eta^{n-1}}{\Delta t^2}$ on Σ

ii. $\rho_w h_s \dfrac{\tilde{\eta}_k - 2\eta^n + \eta^{n-1}}{\Delta t^2} + b\tilde{\eta}_k = p_k + p_{ext}^{n+1}$ on Σ

iii. $\eta_k = \omega\tilde{\eta}_k + (1-\omega)\eta_{k-1}$

•equivalent to a fixed point algorithm on η^{n+1}.

Proposition 2

The Dirichlet-Neumann iterative algorithm converges iff

$$0 < \omega < \frac{2+\epsilon}{1+\rho_f \mu_{max}/\varrho_s h_s + \epsilon} \qquad \text{where } \epsilon = b\Delta t^2/\varrho_s h_s$$

- In the limit $\Delta t \to 0$, whenever the explicit algorithm diverges ($\rho_f \mu_{max} > \rho_s h_s$), the D-N iterative method needs a relaxation parameter strictly smaller than 1 to converge.

- The algorithm needs more relaxation for ρ_s/ρ_f small and μ_{max} large.

Proposition 2

The Dirichlet-Neumann iterative algorithm converges iff

$$0 < \omega < \frac{2+\epsilon}{1+\rho_f \mu_{max}/\varrho_s h_s + \epsilon} \qquad \text{where } \epsilon = b\Delta t^2/\varrho_s h_s$$

- In the limit $\Delta t \to 0$, whenever the explicit algorithm diverges ($\rho_f \mu_{max} > \rho_s h_s$), the D-N iterative method needs a relaxation parameter strictly smaller than 1 to converge.

- The algorithm needs more relaxation for ρ_s/ρ_f small and μ_{max} large.

Proposition 2

The Dirichlet-Neumann iterative algorithm converges iff

$$0 < \omega < \frac{2+\epsilon}{1+\rho_f \mu_{max}/\varrho_s h_s + \epsilon} \qquad \text{where } \epsilon = b\Delta t^2/\varrho_s h_s$$

- In the limit $\Delta t \to 0$, whenever the explicit algorithm diverges ($\rho_f \mu_{max} > \rho_s h_s$), the D-N iterative method needs a relaxation parameter strictly smaller than 1 to converge.

- The algorithm needs more relaxation for ρ_s/ρ_f small and μ_{max} large.

Neumann-Dirichlet subiterations

given an initial guess η_0^{n+1}, *we solve for each* $k = 1, 2, \ldots$

i. $\phi_k = \rho_s h_s \dfrac{\eta_{k-1} - 2\eta^n + \eta^{n-1}}{\Delta t^2} + a\eta_{k-1} - p_{ext}^{n+1}$ in Σ

ii. $\Delta p_k = 0$ in Ω_F

$p_k = \phi_k$ on Σ,

iii. $\tilde{\eta}_k = \Delta t \mathbf{u}_k \cdot \mathbf{n} + \eta^n$ in Σ

iv. $\eta_k = \omega\tilde{\eta}_k + (1-\omega)\eta_{k-1}$.

- Again, this iterative algorithm can be seen as a fixed point method on η^{n+1}.

Neumann-Dirichlet subiterations

given an initial guess η_0^{n+1}, *we solve for each* $k = 1, 2, \ldots$

i. $\phi_k = \rho_s h_s \dfrac{\eta_{k-1} - 2\eta^n + \eta^{n-1}}{\Delta t^2} + a\eta_{k-1} - p_{ext}^{n+1}$ in Σ

ii. $\Delta p_k = 0$ in Ω_F

$p_k = \phi_k$ on Σ,

iii. $\tilde{\eta}_k = \Delta t \mathbf{u}_k \cdot \mathbf{n} + \eta^n$ in Σ

iv. $\eta_k = \omega\tilde{\eta}_k + (1-\omega)\eta_{k-1}$.

•Again, this iterative algorithm can be seen as a fixed point method on η^{n+1}.

Proposition 3

The N-D iterative method converges to the solution of BDF1+IE if and only if, for all $i = 1, 2, \ldots,$

$$0 < \omega < \frac{2\rho_f}{\rho_f + (\rho_s h_s + a\Delta t^2)/\mu_i}$$

- At the continuous level, $\inf_i \mu_i = 0$.

- At the discrete level, $\mu_{min} = O(h)$. Hence, the relaxation parameter needed to have convergence tends to zero with h !!

Proposition 3

The N-D iterative method converges to the solution of BDF1+IE if and only if, for all $i = 1, 2, \ldots,$

$$0 < \omega < \frac{2\rho_f}{\rho_f + (\rho_s h_s + a\Delta t^2)/\mu_i}$$

- At the continuous level, $\inf_i \mu_i = 0$.

- At the discrete level, $\mu_{min} = O(h)$. Hence, the relaxation parameter needed to have convergence tends to zero with h !!

Proposition 3

The N-D iterative method converges to the solution of BDF1+IE if and only if, for all $i = 1, 2, \ldots,$

$$0 < \omega < \frac{2\rho_f}{\rho_f + (\rho_s h_s + a\Delta t^2)/\mu_i}$$

- At the continuous level, $\inf_i \mu_i = 0$.

- At the discrete level, $\mu_{min} = O(h)$. Hence, the relaxation parameter needed to have convergence tends to zero with h !!

Back to the non linear problem - ongoing research

- Implicit coupling is needed for stability purposes. The non-linear problem can be written at each time step as an interface equation on the structure displacement and velocity
- Several techniques have been proposed to solve efficiently the coupled non-linear problem:
  - Fixed point iterations with Aitken extrapolation [S. Deparis, M. Fernandez]
  - Non linear Domain Decomposition algorithms (DN, ND, NN) [M. Discacciati, S. Deparis, A. Quarteroni]
  - Exact Newton on the interface equation [M. Fernandez, Moubachir] + GMRES to solve the tangent operator
  - Quasi-Newton; tangent operator approximated with the added mass model [J.F. Gerbeau, M. Vidrascu]
- There is space left for further improvement.

Back to the non linear problem - ongoing research

- Implicit coupling is needed for stability purposes. The non-linear problem can be written at each time step as an interface equation on the structure displacement and velocity
- Several techniques have been proposed to solve efficiently the coupled non-linear problem:
  - Fixed point iterations with Aitken extrapolation [S. Deparis, M. Fernandez]
  - Non linear Domain Decomposition algorithms (DN, ND, NN) [M. Discacciati, S. Deparis, A. Quarteroni]
  - Exact Newton on the interface equation [M. Fernandez, Moubachir] + GMRES to solve the tangent operator
  - Quasi-Newton; tangent operator approximated with the added mass model [J.F. Gerbeau, M. Vidrascu]
- There is space left for further improvement.

Back to the non linear problem - ongoing research

- Implicit coupling is needed for stability purposes. The non-linear problem can be written at each time step as an interface equation on the structure displacement and velocity
- Several techniques have been proposed to solve efficiently the coupled non-linear problem:
  - Fixed point iterations with Aitken extrapolation [S. Deparis, M. Fernandez]
  - Non linear Domain Decomposition algorithms (DN, ND, NN) [M. Discacciati, S. Deparis, A. Quarteroni]
  - Exact Newton on the interface equation [M. Fernandez, Moubachir] + GMRES to solve the tangent operator
  - Quasi-Newton; tangent operator approximated with the added mass model [J.F. Gerbeau, M. Vidrascu]
- There is space left for further improvement.

Back to the non linear problem - ongoing research

- Implicit coupling is needed for stability purposes. The non-linear problem can be written at each time step as an interface equation on the structure displacement and velocity
- Several techniques have been proposed to solve efficiently the coupled non-linear problem:
  - Fixed point iterations with Aitken extrapolation [S. Deparis, M. Fernandez]
  - Non linear Domain Decomposition algorithms (DN, ND, NN) [M. Discacciati, S. Deparis, A. Quarteroni]
  - Exact Newton on the interface equation [M. Fernandez, Moubachir] + GMRES to solve the tangent operator
  - Quasi-Newton; tangent operator approximated with the added mass model [J.F. Gerbeau, M. Vidrascu]
- There is space left for further improvement.

Back to the non linear problem - ongoing research

- Implicit coupling is needed for stability purposes. The non-linear problem can be written at each time step as an interface equation on the structure displacement and velocity
- Several techniques have been proposed to solve efficiently the coupled non-linear problem:
  - Fixed point iterations with Aitken extrapolation [S. Deparis, M. Fernandez]
  - Non linear Domain Decomposition algorithms (DN, ND, NN) [M. Discacciati, S. Deparis, A. Quarteroni]
  - Exact Newton on the interface equation [M. Fernandez, Moubachir] + GMRES to solve the tangent operator
  - Quasi-Newton; tangent operator approximated with the added mass model [J.F. Gerbeau, M. Vidrascu]
- There is space left for further improvement.

Back to the non linear problem - ongoing research

- Implicit coupling is needed for stability purposes. The non-linear problem can be written at each time step as an interface equation on the structure displacement and velocity
- Several techniques have been proposed to solve efficiently the coupled non-linear problem:
  - Fixed point iterations with Aitken extrapolation [S. Deparis, M. Fernandez]
  - Non linear Domain Decomposition algorithms (DN, ND, NN) [M. Discacciati, S. Deparis, A. Quarteroni]
  - Exact Newton on the interface equation [M. Fernandez, Moubachir] + GMRES to solve the tangent operator
  - Quasi-Newton; tangent operator approximated with the added mass model [J.F. Gerbeau, M. Vidrascu]
- There is space left for further improvement.

Numerical results – pressure pulse in a pipe

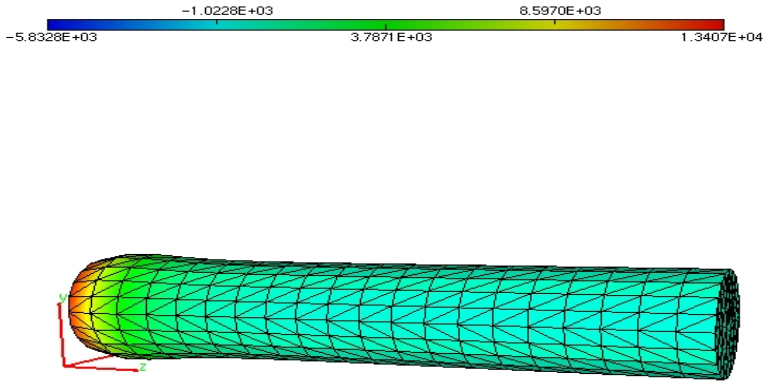

(A. Moura, MOX)

Solved with linear 3D elasticity + exact Newton iterations + Homogeneous Neumann b.cs on the outflow section

Numerical results – Carotid bifurcation

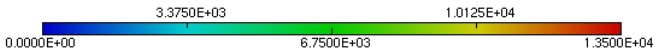

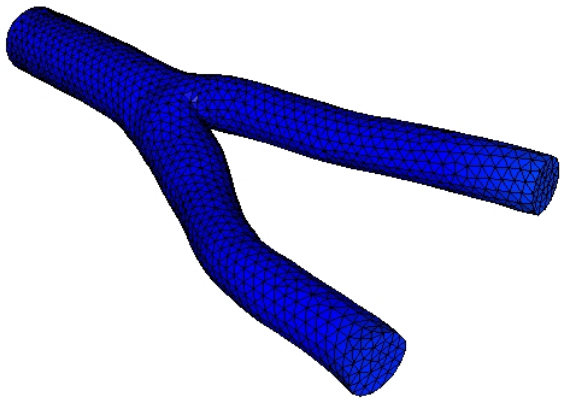

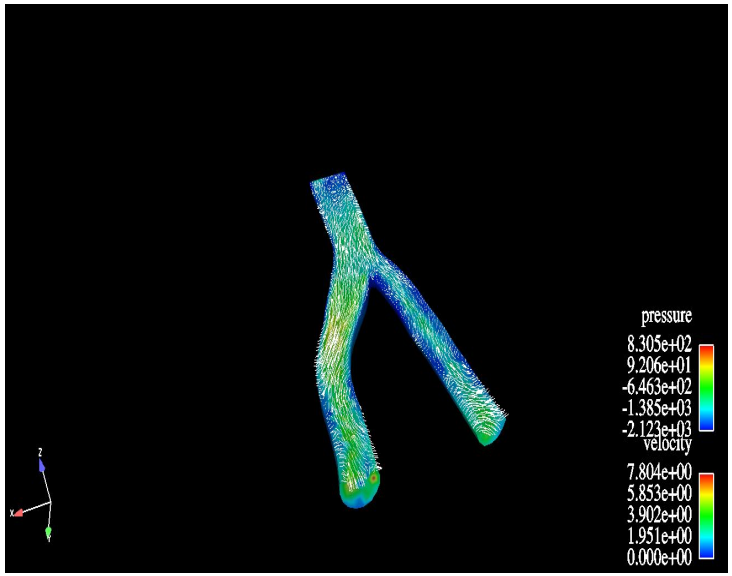

(A. Moura, MOX)

Solved with linear 3D elasticity + exact Newton iterations + Homogeneous Neumann b.cs on the outflow sections

Outline

1. Introduction
2. Mathematical problem
   - Governing equations
   - Global weak formulation
   - Energy inequality
3. Numerical approximation and stability analysis
   - ALE framework
   - Partitioned algorithms
   - Added mass effect
4. Absorbing boundary conditions
   - 1D hyperbolic model
   - Absorbing boundary conditions
5. Numerical results

1D hyperbolic model

- The fluid-structure problem behaves like a propagative system
- For a cylindrical pipe, the propagative nature can be seen by integrating the equations on each transversal section.

Averaged variables

flux: $$Q(z) = \int_{S(z)} u_z$$

Area: $$A(Z) = |S(z)|$$

mean pressure: $$\bar{p}(z) = \frac{1}{A(z)} \int_{S(z)} p$$

1D hyperbolic model

- The fluid-structure problem behaves like a propagative system
- For a cylindrical pipe, the propagative nature can be seen by integrating the equations on each transversal section.

Averaged variables

flux: $$Q(z) = \int_{S(z)} u_z$$

Area: $$A(Z) = |S(z)|$$

mean pressure: $$\bar{p}(z) = \frac{1}{A(z)} \int_{S(z)} p$$

1D hyperbolic model

- The fluid-structure problem behaves like a propagative system
- For a cylindrical pipe, the propagative nature can be seen by integrating the equations on each transversal section.

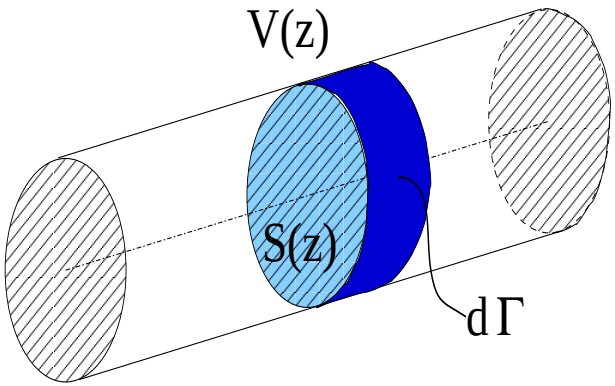

Averaged variables

flux: $$Q(z) = \int_{S(z)} u_z$$

Area: $$A(Z) = |S(z)|$$

mean pressure: $$\bar{p}(z) = \frac{1}{A(z)} \int_{S(z)} p$$

1D hyperbolic model

Solve for $z \in (a,b),\ t > 0$

$$\begin{cases} \dfrac{\partial A}{\partial t} + \dfrac{\partial Q}{\partial z} = 0, & \text{(mass equation)} \\ \dfrac{\partial Q}{\partial t} + \dfrac{\partial}{\partial z}\left(\dfrac{Q^2}{A}\right) + \dfrac{A}{\rho}\dfrac{\partial \overline{p}}{\partial z} = -K_r \dfrac{Q}{A}, & \text{(momentum equation)} \end{cases}$$

$$\overline{p}(A; A_0, \beta) = \beta \frac{\sqrt{A} - \sqrt{A_0}}{A_0} \quad \text{with} \quad \beta = \frac{\sqrt{\pi} h_0 E}{1 - \nu^2} \qquad \text{(algebraic law)}$$

- It is a full hyperbolic system with characteristic speeds $\lambda_{1,2} = \frac{Q}{A} \pm c$, and $c^2 = \frac{A}{\rho}\frac{\partial \overline{p}}{\partial A}$ (in physiological conditions $\lambda_1 > 0$ and $\lambda_2 < 0$)
- It admits the characteristic variables $W_{1,2} = \frac{Q}{A} \pm \int_{A_0}^{A} \frac{c(s)}{s} ds$

1D hyperbolic model

Solve for $z \in (a,b),\ t > 0$

$$\begin{cases} \dfrac{\partial A}{\partial t} + \dfrac{\partial Q}{\partial z} = 0, & \text{(mass equation)} \\ \dfrac{\partial Q}{\partial t} + \dfrac{\partial}{\partial z}\left(\dfrac{Q^2}{A}\right) + \dfrac{A}{\rho}\dfrac{\partial \overline{p}}{\partial z} = -K_r \dfrac{Q}{A}, & \text{(momentum equation)} \end{cases}$$

$$\overline{p}(A; A_0, \beta) = \beta \frac{\sqrt{A} - \sqrt{A_0}}{A_0} \quad \text{with} \quad \beta = \frac{\sqrt{\pi} h_0 E}{1 - \nu^2} \qquad \text{(algebraic law)}$$

- It is a full hyperbolic system with characteristic speeds $\lambda_{1,2} = \frac{Q}{A} \pm c$, and $c^2 = \frac{A}{\rho}\frac{\partial \overline{p}}{\partial A}$ (in physiological conditions $\lambda_1 > 0$ and $\lambda_2 < 0$)
- It admits the characteristic variables $W_{1,2} = \frac{Q}{A} \pm \int_{A_0}^{A} \frac{c(s)}{s} ds$

1D hyperbolic model

Solve for $z \in (a, b),\ t > 0$

$$\begin{cases} \dfrac{\partial A}{\partial t} + \dfrac{\partial Q}{\partial z} = 0, & \text{(mass equation)} \\ \dfrac{\partial Q}{\partial t} + \dfrac{\partial}{\partial z}\left(\dfrac{Q^2}{A}\right) + \dfrac{A}{\rho}\dfrac{\partial \overline{p}}{\partial z} = -K_r \dfrac{Q}{A}, & \text{(momentum equation)} \end{cases}$$

$$\overline{p}(A; A_0, \beta) = \beta \frac{\sqrt{A} - \sqrt{A_0}}{A_0} \quad \text{with} \quad \beta = \frac{\sqrt{\pi} h_0 E}{1 - \nu^2} \qquad \text{(algebraic law)}$$

- It is a full hyperbolic system with characteristic speeds $\lambda_{1,2} = \frac{Q}{A} \pm c$, and $c^2 = \frac{A}{\rho}\frac{\partial \overline{p}}{\partial A}$ (in physiological conditions $\lambda_1 > 0$ and $\lambda_2 < 0$)
- It admits the characteristic variables $W_{1,2} = \frac{Q}{A} \pm \int_{A_0}^{A} \frac{c(s)}{s} ds$

Absorbing boundary condition

- The condition $W_2 = 0$ is an absorbing boundary condition for the 1D model (no information entering the domain from the right)
- Idea: apply the same condition to the 3D problem

Absorbing boundary condition

$$W_2(Q, \bar{p}) = \frac{Q}{A} - \frac{2}{\sqrt{\varrho_0^s}} \left(\sqrt{\bar{p} + \beta\sqrt{A_0}} - \sqrt{\beta\sqrt{A_0}} \right) = 0 \qquad \text{on } \Gamma_{out}$$

- Use an explicit approach:
  - either impose a Neumann boundary condition $\sigma_f^{n+1} \cdot \mathbf{n} = \bar{p}^{n+1}\mathbf{n}$ such that $W_2(\bar{p}^{n+1}, Q^n) = 0$
  - or impose a outflow flux Q^{n+1} such that $W_2(Q^{n+1}, \bar{p}^n)$ by a Lagrange Multiplier

Absorbing boundary condition

- The condition $W_2 = 0$ is an absorbing boundary condition for the 1D model (no information entering the domain from the right)
- Idea: apply the same condition to the 3D problem

Absorbing boundary condition

$$W_2(Q, \bar{p}) = \frac{Q}{A} - \frac{2}{\sqrt{\varrho_0^s}} \left(\sqrt{\bar{p} + \beta\sqrt{A_0}} - \sqrt{\beta\sqrt{A_0}} \right) = 0 \qquad \text{on } \Gamma_{out}$$

- Use an explicit approach:
  - either impose a Neumann boundary condition $\sigma_f^{n+1} \cdot \mathbf{n} = \bar{p}^{n+1}\mathbf{n}$ such that $W_2(\bar{p}^{n+1}, Q^n) = 0$
  - or impose a outflow flux Q^{n+1} such that $W_2(Q^{n+1}, \bar{p}^n)$ by a Lagrange Multiplier

Absorbing boundary condition

- The condition $W_2 = 0$ is an absorbing boundary condition for the 1D model (no information entering the domain from the right)
- Idea: apply the same condition to the 3D problem

Absorbing boundary condition

$$W_2(Q, \bar{p}) = \frac{Q}{A} - \frac{2}{\sqrt{\varrho_0^s}} \left(\sqrt{\bar{p} + \beta\sqrt{A_0}} - \sqrt{\beta\sqrt{A_0}} \right) = 0 \qquad \text{on } \Gamma_{out}$$

- Use an explicit approach:
  - either impose a Neumann boundary condition $\boldsymbol{\sigma}_{\mathbf{f}}^{\mathbf{n+1}} \cdot \mathbf{n} = \bar{p}^{n+1}\mathbf{n}$ such that $W_2(\bar{p}^{n+1}, Q^n) = 0$
  - or impose a outflow flux Q^{n+1} such that $W_2(Q^{n+1}, \bar{p}^n)$ by a Lagrange Multiplier

Absorbing boundary condition

- The condition $W_2 = 0$ is an absorbing boundary condition for the 1D model (no information entering the domain from the right)
- Idea: apply the same condition to the 3D problem

Absorbing boundary condition

$$W_2(Q, \bar{p}) = \frac{Q}{A} - \frac{2}{\sqrt{\varrho_0^s}} \left(\sqrt{\bar{p} + \beta\sqrt{A_0}} - \sqrt{\beta\sqrt{A_0}} \right) = 0 \qquad \text{on } \Gamma_{out}$$

- Use an explicit approach:
  - either impose a Neumann boundary condition $\boldsymbol{\sigma}_{\mathbf{f}}^{\mathbf{n+1}} \cdot \mathbf{n} = \bar{p}^{n+1}\mathbf{n}$ such that $W_2(\bar{p}^{n+1}, Q^n) = 0$
  - or impose a outflow flux Q^{n+1} such that $W_2(Q^{n+1}, \bar{p}^n)$ by a Lagrange Multiplier

Outline

1. Introduction
2. Mathematical problem
   - Governing equations
   - Global weak formulation
   - Energy inequality
3. Numerical approximation and stability analysis
   - ALE framework
   - Partitioned algorithms
   - Added mass effect
4. Absorbing boundary conditions
   - 1D hyperbolic model
   - Absorbing boundary conditions
5. Numerical results

Numerical results – pressure pulse in a pipe

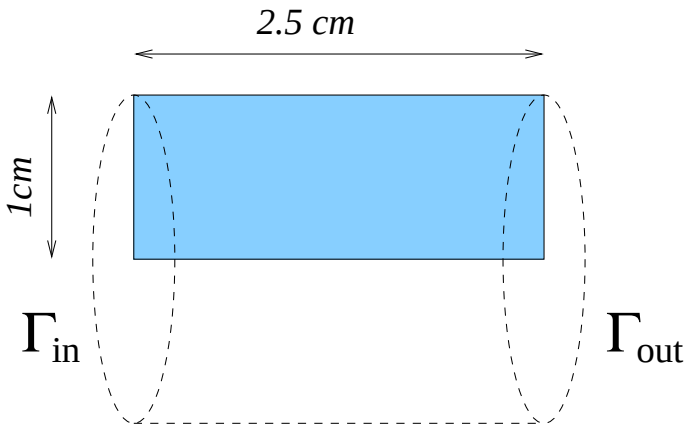

- Axisymmetric formulation
- Algebraic structure law
- Inlet pressure:

$$P_{in} = \begin{cases} 5000 \frac{dyne}{cm^3} & t \leq 5ms \\ 0 & t > 5ms \end{cases}$$

- mean pressure on cross section at $x = 1.4\,cm$
- Comparison between absorbing and non-absorbing (homogeneous Neumann) boundary conditions

Numerical results – pressure pulse in a pipe

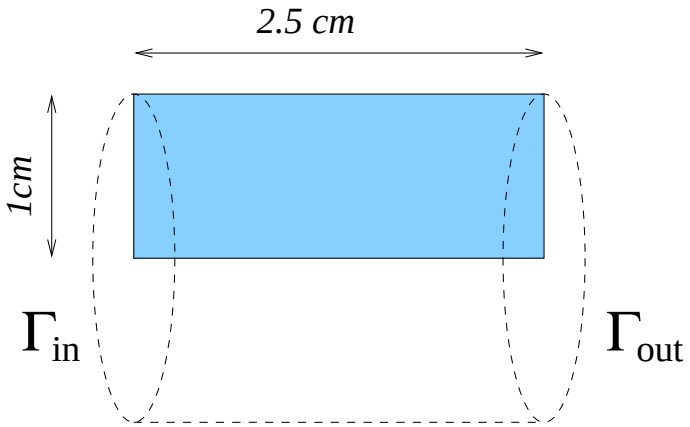

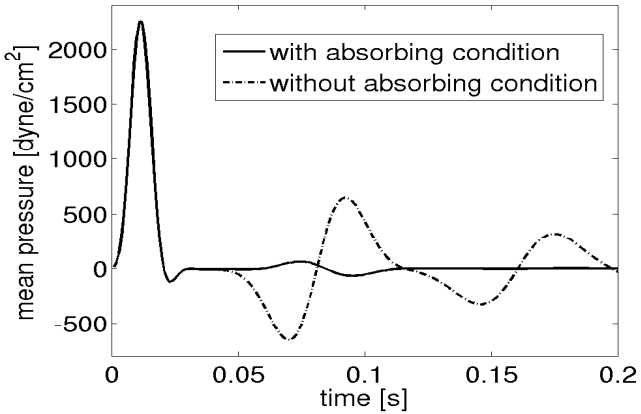

- Axisymmetric formulation
- Algebraic structure law
- Inlet pressure:

$$P_{in} = \begin{cases} 5000 \frac{dyne}{cm^3} & t \leq 5ms \\ 0 & t > 5ms \end{cases}$$

- mean pressure on cross section at $x = 1.4\,cm$
- Comparison between absorbing and non-absorbing (homogeneous Neumann) boundary conditions

Numerical results – Womersley flow

- A very well known analytical solution in vascular dynamics is the Womersley profile
  - Prototype of pulsatile flow
  - Feature flow reversal
- Same geometry as before but with rigid wall
- Inlet pulsatile flow rate

$$Q_{in} = \sin(2\pi t) cm^3/sec$$

- Outlet stress free cond.

(C. Vergara, MOX)

- Axial velocity profile on (any) cross section

Numerical results – Womersley flow

- A very well known analytical solution in vascular dynamics is the Womersley profile
  - Prototype of pulsatile flow
  - Feature flow reversal
- Same geometry as before but with rigid wall
- Inlet pulsatile flow rate

$$Q_{in} = \sin(2\pi t) cm^3/sec$$

- Outlet stress free cond.

(C. Vergara, MOX)

- Axial velocity profile on (any) cross section

Numerical results – Womersley flow

- A very well known analytical solution in vascular dynamics is the Womersley profile
  - Prototype of pulsatile flow
  - Feature flow reversal
- Same geometry as before but with rigid wall
- Inlet pulsatile flow rate

$$Q_{in} = \sin(2\pi t) cm^3/sec$$

- Outlet stress free cond.

(C. Vergara, MOX)

- Axial velocity profile on (any) cross section

Numerical results – Womersley flow

- A very well known analytical solution in vascular dynamics is the Womersley profile
  - Prototype of pulsatile flow
  - Feature flow reversal
- Same geometry as before but with rigid wall
- Inlet pulsatile flow rate

$$Q_{in} = \sin(2\pi t) cm^3/sec$$

- Outlet stress free cond.

(C. Vergara, MOX)

•Axial velocity profile on (any) cross section

Numerical results – Womersley flow

- A very well known analytical solution in vascular dynamics is the Womersley profile
  - Prototype of pulsatile flow
  - Feature flow reversal
- Same geometry as before but with rigid wall
- Inlet pulsatile flow rate

$$Q_{in} = \sin(2\pi t) cm^3/sec$$

- Outlet stress free cond.

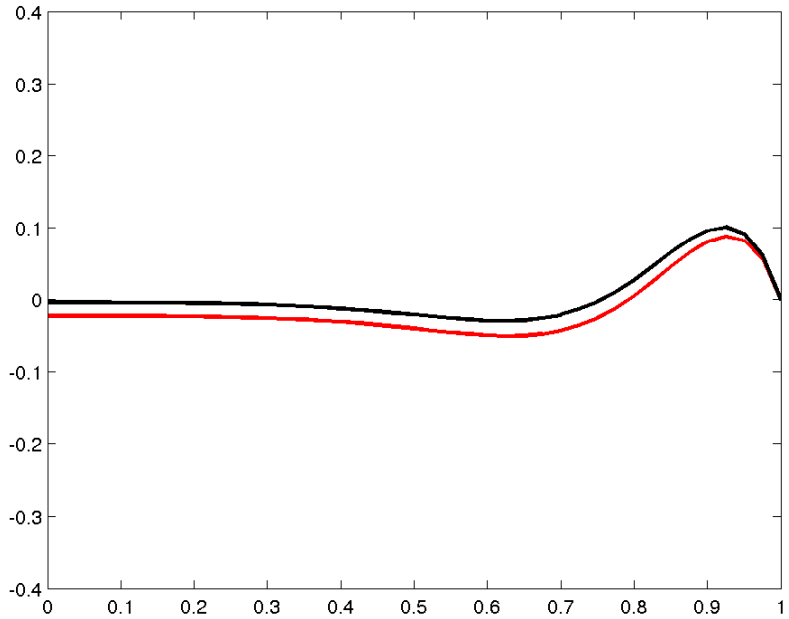

(C. Vergara, MOX)

•Axial velocity profile on (any) cross section

Numerical results – Fluid-structure equivalent

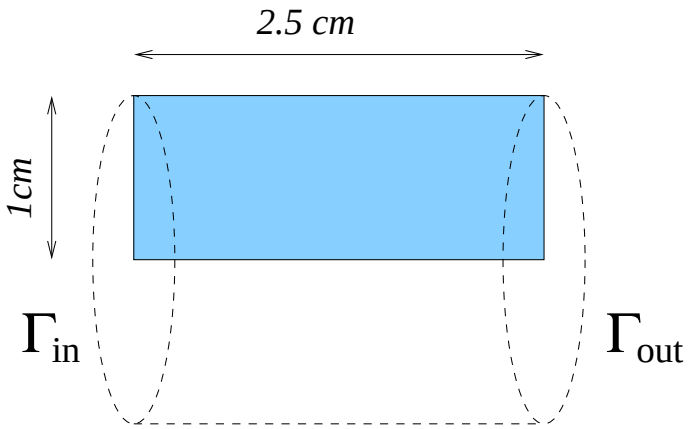

- Axisymmetric formulation
- Algebraic structure law
- Inlet flow rate
  $Q_i n = \sin(2\pi t)$
- Outlet absorbing boundary conditions

(C. Vergara, MOX)

- Axial velocity profile on Γ_{out}

Numerical results – Fluid-structure equivalent

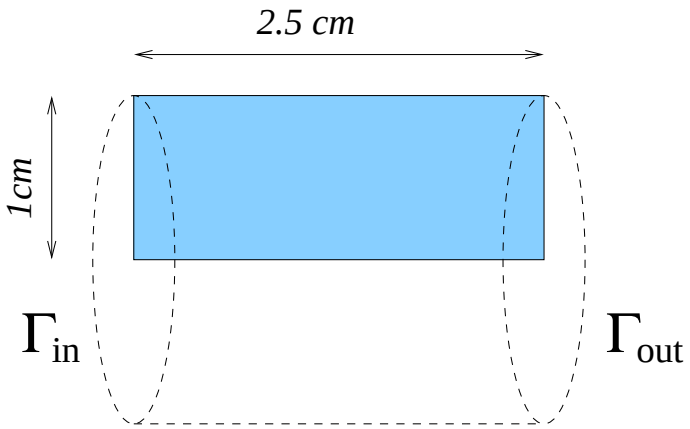

- Axisymmetric formulation
- Algebraic structure law
- Inlet flow rate
  $Q_i n = \sin(2\pi t)$
- Outlet absorbing boundary conditions

(C. Vergara, MOX)

- Axial velocity profile on Γ_{out}

Numerical results – Fluid-structure equivalent

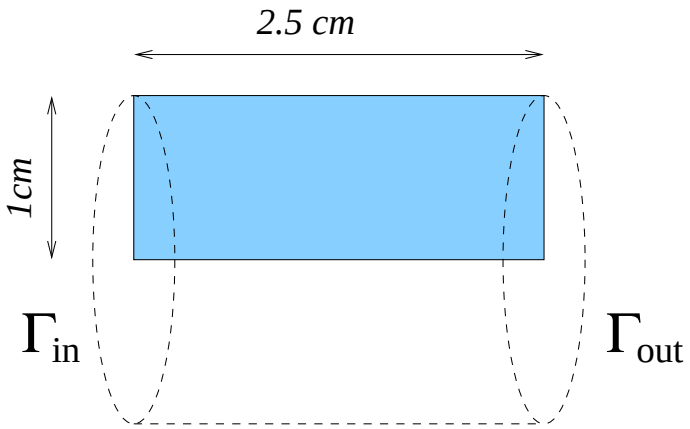

- Axisymmetric formulation
- Algebraic structure law
- Inlet flow rate
  $Q_i n = \sin(2\pi t)$
- Outlet absorbing boundary conditions

(C. Vergara, MOX)

- Axial velocity profile on Γ_{out}

Numerical results – Fluid-structure equivalent

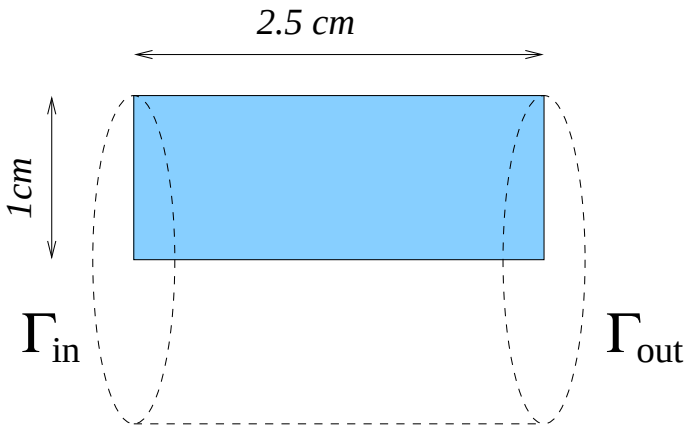

- Axisymmetric formulation
- Algebraic structure law
- Inlet flow rate
  $Q_i n = \sin(2\pi t)$
- Outlet absorbing boundary conditions

(C. Vergara, MOX)

- Axial velocity profile on Γ_{out}

Numerical results – Fluid-structure equivalent

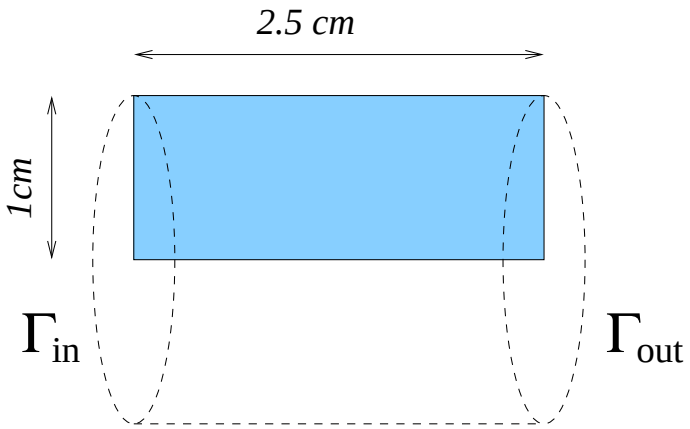

- Axisymmetric formulation
- Algebraic structure law
- Inlet flow rate
  $Q_i n = \sin(2\pi t)$
- Outlet absorbing boundary conditions

(C. Vergara, MOX)

- Axial velocity profile on Γ_{out}

Numerical results – Fluid-structure equivalent

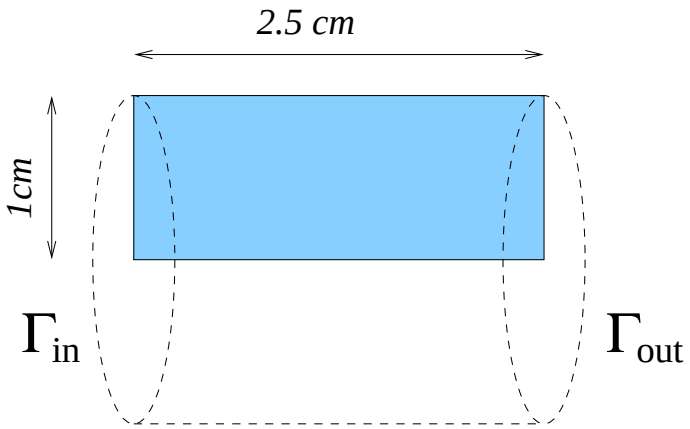

- Axisymmetric formulation
- Algebraic structure law
- Inlet flow rate
  $Q_i n = \sin(2\pi t)$
- Outlet absorbing boundary conditions

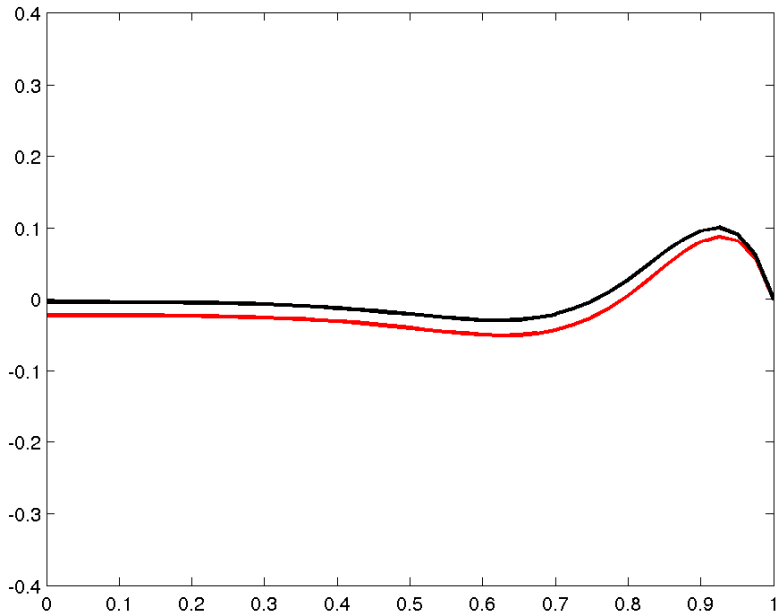

(C. Vergara, MOX)

- Axial velocity profile on Γ_{out}

Numerical results – Fluid-structure equivalent

- The fluid-structure solution on Γ_{out} looks delayed by $\approx 9\,ms$.
- We superpose in the plot the Womersley solutions delayed by $9\,ms$

(C. Vergara, MOX)

Black: Womersley profile $u_W(t)$

Red: Fluid-structure solution $u_{FS}(t)$

Blue: Delayed Womersley sol. $u_W(t - 9ms)$

Numerical results – Fluid-structure equivalent

- The fluid-structure solution on Γ_{out} looks delayed by $\approx 9\,ms$.
- We superpose in the plot the Womersley solutions delayed by $9\,ms$

(C. Vergara, MOX)

Black: Womersley profile $u_W(t)$

Red: Fluid-structure solution $u_{FS}(t)$

Blue: Delayed Womersley sol. $u_W(t - 9ms)$

Numerical results – Fluid-structure equivalent

- The fluid-structure solution on Γ_{out} looks delayed by $\approx 9\,ms$.
- We superpose in the plot the Womersley solutions delayed by $9\,ms$

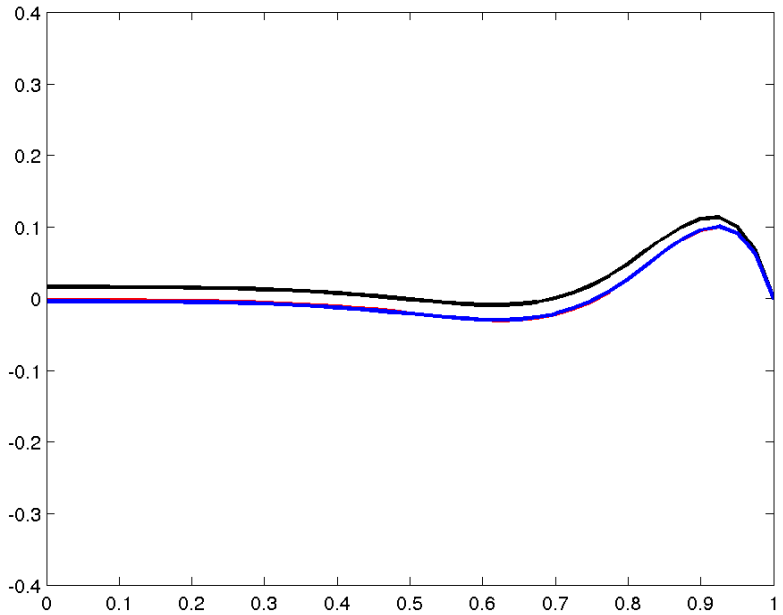

(C. Vergara, MOX)

Black: Womersley profile $u_W(t)$

Red: Fluid-structure solution $u_{FS}(t)$

Blue: Delayed Womersley sol. $u_W(t - 9ms)$

Numerical results – A more realistic case

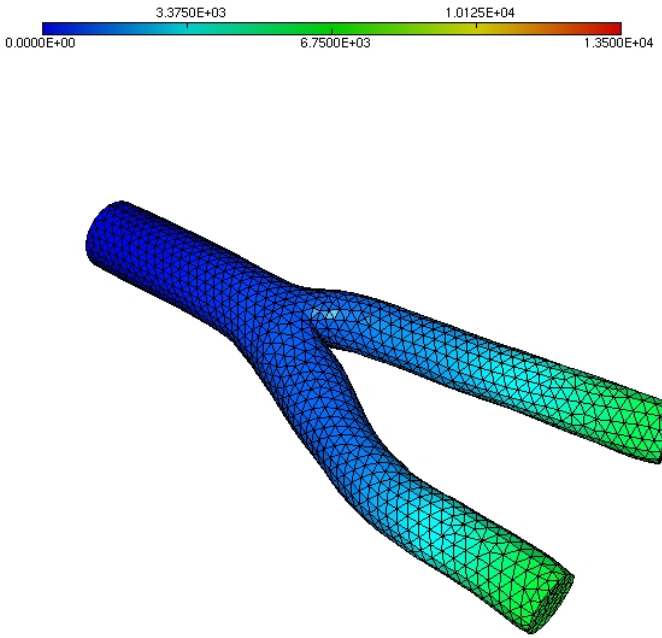

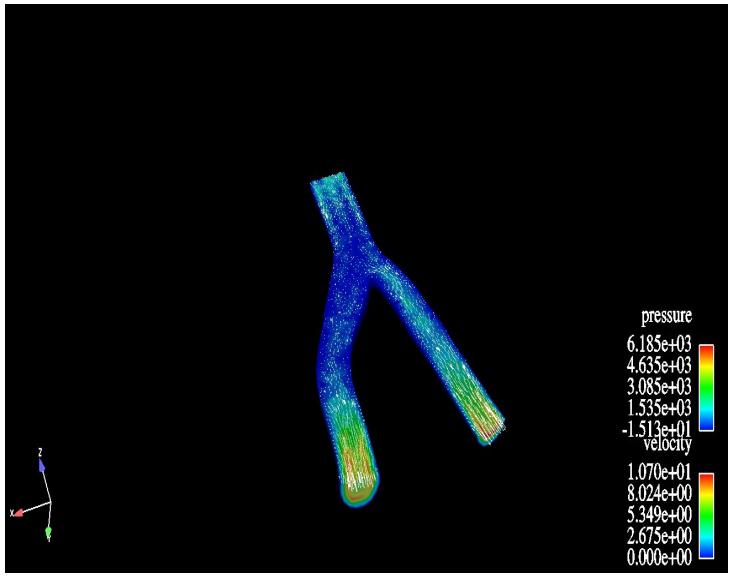

(A. Moura, MOX)

Solved with linear 3D elasticity + exact Newton iterations + absorbing boundary conditions